UNCLASSIFIED

Response of Materials to Laser Radiation: A Short Course

J. T. SCHRIEMPF

Metal Physics Branch
Metallurgy Division

July 10, 1974
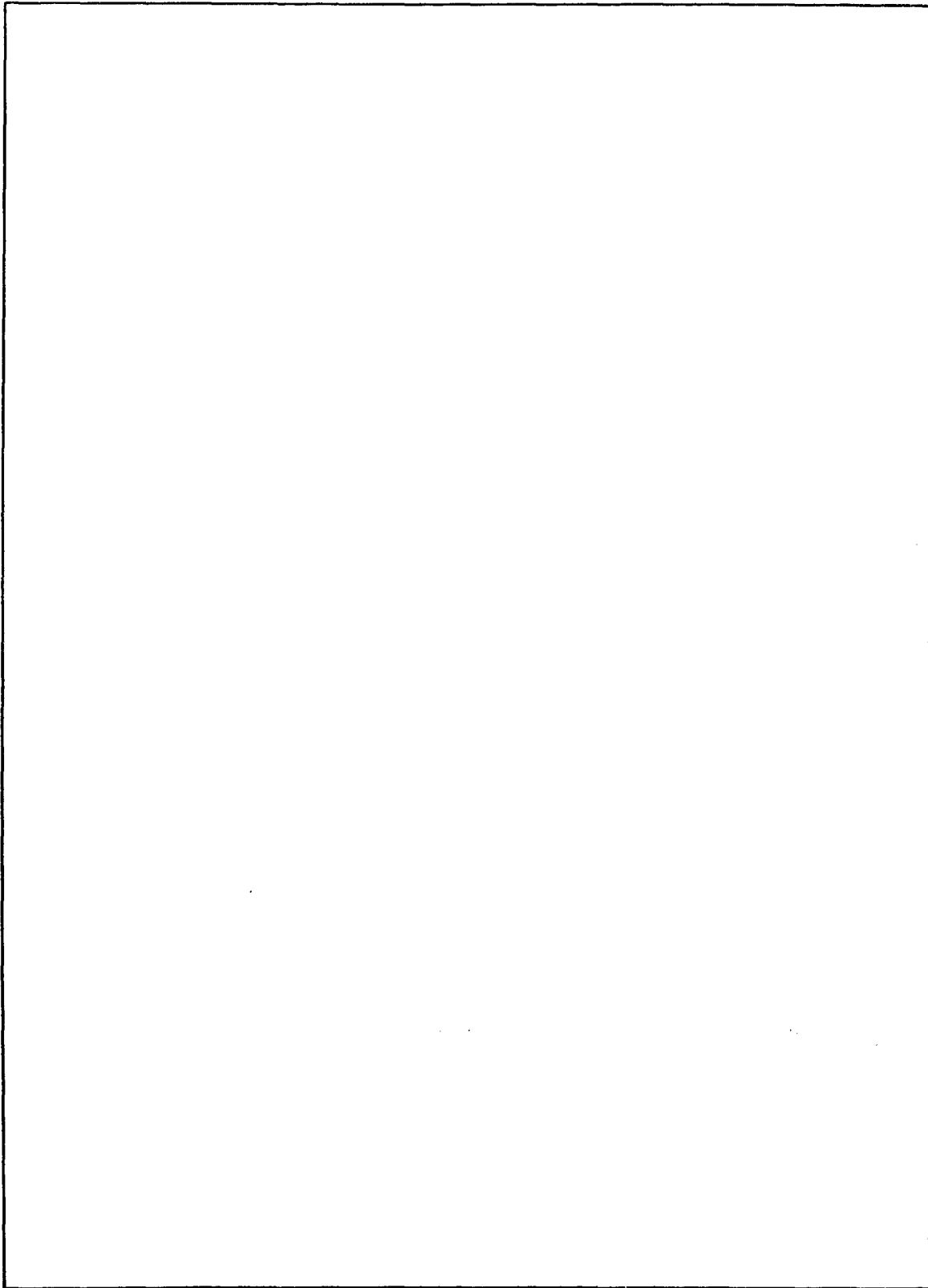
NAVAL RESEARCH LABORATORY
Washington, D.C.

Approved for public release; distribution unlimited.

UNCLASSIFIED

REPORT DOCUMENTATION PAGE		READ INSTRUCTIONS BEFORE COMPLETING FORM
1. REPORT NUMBER NRL Report 7728	2. GOVT ACCESSION NO.	3. RECIPIENT'S CATALOG NUMBER
4. TITLE (and Subtitle) RESPONSE OF MATERIALS TO LASER RADIATION: A SHORT COURSE		5. TYPE OF REPORT & PERIOD COVERED Summary report on one phase of a continuing NRL problem.
		6. PERFORMING ORG. REPORT NUMBER
7. AUTHOR(s) J. T. Schriempf		8. CONTRACT OR GRANT NUMBER(s)
9. PERFORMING ORGANIZATION NAME AND ADDRESS Naval Research Laboratory Washington, D.C. 20375		10. PROGRAM ELEMENT, PROJECT, TASK AREA & WORK UNIT NUMBERS NRL Problem M01-26 RR 022-01-46-5433
11. CONTROLLING OFFICE NAME AND ADDRESS Department of the Navy Office of Naval Research Arlington, Va. 22217		12. REPORT DATE July 10, 1974
		13. NUMBER OF PAGES 77
14. MONITORING AGENCY NAME & ADDRESS(if different from Controlling Office)		15. SECURITY CLASS. (of this report) Unclassified
		15a. DECLASSIFICATION/DOWNGRADING SCHEDULE

16. DISTRIBUTION STATEMENT (of this Report)

Approved for public release; distribution unlimited.

17. DISTRIBUTION STATEMENT (of the abstract entered in Block 20, if different from Report)

18. SUPPLEMENTARY NOTES

19. KEY WORDS (Continue on reverse side if necessary and identify by block number)

Laser	Pulsed laser effects
Laser-material interaction	Laser-supported detonation waves
Laser coupling	Coupling coefficients
Coherent radiation effects on materials	Thermal response to laser radiation
Optical absorptance	

20. ABSTRACT (Continue on reverse side if necessary and identify by block number)

A tutorial discussion of the response of materials to laser radiation is presented, with emphasis on simple, intuitive models. Topics discussed include optical reflectivity of metals at IR wavelengths, laser-induced heat flow in materials, the effects of melting and vaporization, the impulse generated in materials by pulsed radiation, and the influence of the absorption of laser radiation in the blowoff region in front of the irradiated material.

DD FORM 1 JAN 73 1473 EDITION OF 1 NOV 65 IS OBSOLETE
S/N 0102-014-6601 |

i

CONTENTS

PREFACE

This short course on laser effects was developed for a 12-hour series of lectures delivered by the author at the Naval Postgraduate School in the fall of 1973. The lectures were part of Professor John Neighbours' course on solid-state physics, which stressed topics appropriate to an understanding of laser effects by solid state physicists.

The author is grateful to Professor Neighbours for the opportunity to present these lectures and for many valuable discussions during their development. He also wishes to thank Professor Otto Heinz, chairman, and those other members of the Department of Physics and Chemistry of the Naval Postgraduate School, too numerous to mention here, who through their support and hospitality made valuable contributions to this work.

RESPONSE OF MATERIALS TO LASER RADIATION:
A SHORT COURSE

1. LASERS

1.1. Introduction

The word laser, of course, is an acronym for "light amplification by the stimulated emission of radiation," but that is not terribly enlightening. More correctly described a laser is a device for producing light that is almost totally coherent. It works in principle like this: An atom emits a photon of light when it decays from an excited energy state to a lower state; the difference in energy between the two states ΔE determines frequency ν according to

$$\Delta E = h\nu \tag{1}$$

where h is Planck's constant. This is illustrated in Fig. 1.
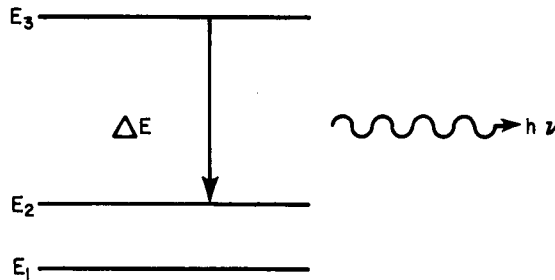
Fig. 1—Energy levels

This is the case for any light source, whether laser, flame, incandescent body, etc. In the conventional light source, atoms emit photons in a random, sporadic manner and spontaneously decay to lower states when excited by heat or electric current. In a laser, on the other hand, the photons are emitted in phase and the electromagnetic radiation thus produced is, more or less, simply a propagating sinusoidal radiation field that can be described on a macroscopic level by, for example,

$$\mathcal{E} = \text{Re} \left[\mathcal{E}_0 e^{-2\pi kz/\lambda} e^{i\omega(t-nz/c)} \right] \tag{2}$$

where

1

$\mathcal{E}$ is the electric field of the radiation

Re stands for the real part of the complex quantity in brackets

$\mathcal{E}_0$ is the maximum amplitude

k is the extinction coefficient; in a vacuum, $k = 0$

z is the direction in which the wave is propagating

λ is the wavelength

t is time

n is the index of refraction; in a vacuum, $n = 1$

c is the velocity of light in vacuum.

Equation (2) is a standard representation of the electric field of a traveling light wave. However, if one measures the electric field at some point in space for light from a conventional source, the sinusoidal variation expressed in Eq. (2) does not appear, for the atoms emitting the light are doing so at random, and the sinusoidal variation due to the emission from each atom is averaged to some time-independent value. This is not true of laser emission, where the individual photons are in phase. Measuring the electric field at a point in space for laser light results in the oscillating $\mathcal{E}$ predicted by Eq. (2).

This coherence is created by taking advantage of stimulated emission in materials in which metastable states can be induced. The lifetime of an atom in an excited state depends on the quantum mechanical selection rules for transition to a lower state, and there are states from which transition to a lower level is extremely improbable. Such states are called metastable, and an atom not disturbed by outside influence will remain in a metastable state for a very long time. If a metastable atom interacts with a photon of frequency such that $\Delta E = h\nu$, where ΔE is the energy difference between the atom's normal and metastable states, stimulated emission will occur. The atom will decay to its normal state by emitting another photon of frequency ν, so that the net result is two photons, and the second photon will have the same phase temporally and spatially as the first.

In a laser, then, one establishes a large number of atoms in metastable states and arranges the optics to increase the likelihood of stimulated emission. Schematically, a typical laser oscillator looks like Fig. 2. The pumping radiation (for example, light from a flashlamp) excites the atoms in the lasing medium (for example, Cr^{+++} ions in ruby). In the decay process (if we have a successful laser), a large number of ions are left in a metastable state; this is called a population inversion. As some atoms begin to decay, they stimulate others to decay. But this alone would not provide a laser, since the emission would occur in random directions. The role of reflection is very important; the photons moving perpendicular to the reflectors pass through the medium many times and on each pass more and more atoms are caused to emit. This results in the build-up of a very strong coherent light signal that travels in a single direction. Useful light output is obtained by making one of the mirrors a partial reflector.
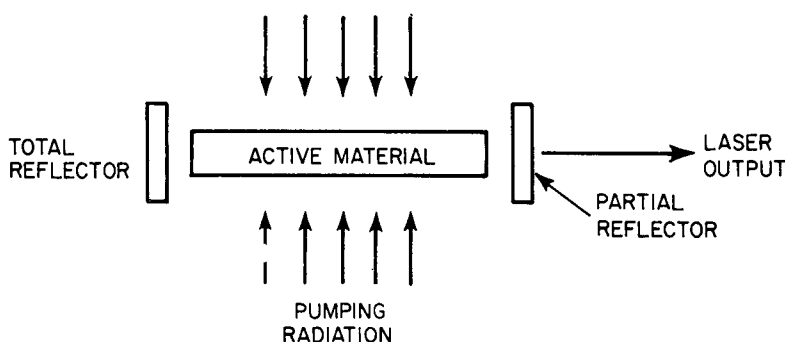
Fig. 2—Schematic representation of a laser

It is interesting to look at a few examples of the intensity of laser light. In a typical ruby laser, the concentration [1] of Cr^{+++} ions is about 2×10^{19} cm^{-3}, and population inversions are of the order of 3×10^{16} cm^{-3}. Crudely speaking, we can think of creating 3×10^{16} quanta/cm^3 in the lasing medium. Since we have arranged the laser so that the output is in a single direction, and since photons move with the speed of light, we obtain $3 \times 10^{16} \times 3 \times 10^{10} = 9 \times 10^{26}$ quanta/cm^{2}s from the laser. For ruby, the lasing wavelength is 6943Å, and since the energy of each quanta is $h\nu$, one can readily calculate that the output is about 2.5×10^8 W/cm^2.

Let us compare this to the power that a hot body, say the sun, emits at the same wavelength with a similar bandwidth. This can be calculated by the use of Planck's radiation law,

$$U_w = \frac{\hbar \omega^3}{\pi^2 c^3} \frac{1}{e^{h\omega/kT}}.$$ (3)

U_w is the energy, per unit volume and per unit bandwidth, radiated by a blackbody at temperature T; k is Boltzmann's constant. The radiation leaves the black-body source at rate c, so the power radiated per unit area of the source, per unit bandwidth, is

$$I_w = \frac{cU_w}{4} = \frac{\hbar w^3}{\pi^2 c^2} \frac{1/4}{e^{h\omega/kT} - 1}.$$ (4)

If we use the sun's temperature of 6000 K, and λ = 6943Å,

$$I_w \approx 2 \times 10^{-5} \text{ erg/cm}^2.$$

For the ruby laser, a typical line width is 3Å, so $\Delta w \approx 1.2 \times 10^{12}$ s^{-1}. Thus the power density at the source is

$$I \approx 2.5 \times 10^7 \text{ erg/cm}^2 \text{ s} \approx 2.5 \text{ W/cm}^2.$$

Thus the power density for comparable narrow-bandwidth, nearly single-frequency light is much greater at a laser source than at a conventional hot-body source, because laser light is coherent.

1.2. Propagation

The propagation of laser light through the atmosphere poses a complex problem and it will not be discussed here. Suffice it to say that, as anyone who has driven on a foggy night certainly realizes, light is certainly scattered in the atmosphere. Lasers of high power density pose even more difficult propagation problems because the high intensity warms the air and creates a density change across the beam. This variation in density refracts the light and causes beam spreading, or "thermal blooming."

Consider briefly the propagation of laser light in free space or in vacuum. Under these ideal conditions, the only change in the power density is due to simple beam divergence. Since the typical laser emits light that is nearly unidirectional, the beam divergence is small. In fact, one feature of a laser is that the divergence is nearly at the diffraction limit, which is of the order of λ/a, where a is the diameter of the output aperture of the laser. For the ruby laser discussed above, this gives a divergence angle of

$$\theta \approx \frac{6943 \times 10^{-8}}{1} \approx 7 \times 10^{-2} \text{ mrad}$$

for, say, a 1-cm aperture. In practice, one needs to go to much trouble to realize this limit of divergence, but it has been done. More commonly, an "off-the-shelf" ruby laser might have a beam divergence of a few mrad.

The newcomer to lasers has usually heard about diffraction-limited beams and the consequent extreme directionality of laser light. He is usually surprised to discover that at long distances from the source these beams have power densities that vary as the reciprocal of the square of the distance, like all radiating sources. To see this, consider a source of power P W, diameter a, and divergence angle θ, as shown in Fig. 3.
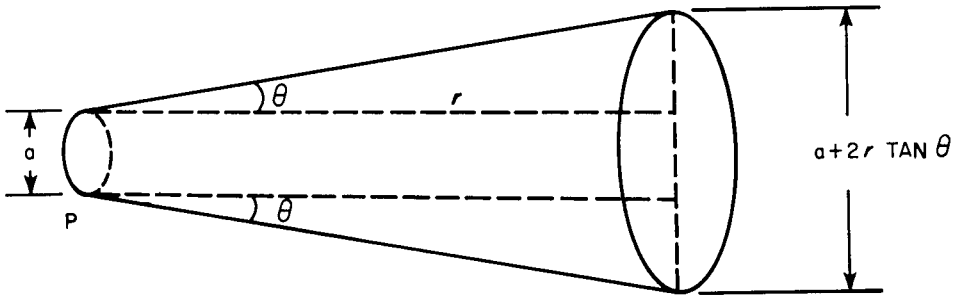

Fig. 3—Simplified sketch of laser beam divergence

At distance r from the source, the power density is

$$I = \frac{P}{\frac{\pi}{4}(a + 2r \tan \theta)^2}$$

or, since θ is very small and $\tan \theta \approx \theta$,

4

$$I = \frac{P}{\frac{\pi}{4}(a + 2r\theta)^2}$$

or

$$I = \frac{P}{\frac{\pi a^2}{4}\left(1 + \frac{2r}{a}\theta\right)^2} \cdot \qquad (5)$$

From this expression it is apparent that for large distances, such that $2r/a \gg 1$,

$$I = \frac{P}{\frac{\pi a^2}{4}\frac{4r^2\theta^2}{a^2}}$$

or

$$I = \frac{P}{\pi r^2 \theta^2}$$

or, since $\theta \approx \lambda/a$,

$$I = \frac{P}{\pi r^2}\frac{a^2}{\lambda^2} \cdot$$

For example, consider a 10-kW beam of 10.6-μm wavelength and 10-cm aperture at 1 mi (i.e., a high-power CO_2 laser);

$$I = \frac{10^4 \times 10^2}{\pi(5280 \times 12 \times 2.54)^2(10 \times 10^{-4})^2}$$

or

$$I \approx 12 \ W/cm^2.$$

From Eq. (5), if we substitute I_0, the power density at the source, for $P/(\pi a^2/4)$ and recall that $\theta \approx \lambda/a$,

$$I = I_0 \frac{1}{\left(1 + 2r\frac{\lambda}{a^2}\right)^2} \cdot \qquad (6)$$

From this expression we can see that if r is small there is little change in power density emitted by the source. The distances at which this is true are referred to as "near field," and the fine details of the beam pattern, such as local variation in intensity, hot spots, etc., are preserved in the near field. It is apparent from Eq. (6) that this near-field distance will be limited to r such that $I \approx I_0$, or

$$\frac{2r\lambda}{a^2} \ll 1$$

or

$$r_{\text{near field}} \ll a^2/\lambda .$$

For lasers with exceptionally good optics that have a Gaussian distribution of power density across the beam, the near field pattern will persist for distances on the order of a^2/λ [2-4].

As a final comment on power densities at distances from laser sources, let us use Eq. (6) to calculate the distance at which the power density is halved:

$$\frac{I}{I_0} = \frac{1}{2} = \frac{1}{\left(1 + \dfrac{2r\lambda}{a^2}\right)^2}$$

and

$$r_{1/2} = \frac{a^2}{2\lambda} (\sqrt{2} - 1) .$$

For our illustration of a CO_2 laser with a 10-cm aperture, $r \approx 680$ ft, or a little more than 0.1 mi.

1.3. Response

The remarks here were not intended to explore lasers or laser propagation at anything beyond the most basic level. They were designed rather to set the stage for the main purpose of these notes, that is, to describe the behavior of materials under irradiation by laser light. A great deal of study is under way in this field, for the application of highly intense light to materials has many uses. In the medical world, for example, lasers are used to "spot-weld" detached retinas. The Ford Motor Company is installing a large laser-computer machine to automatically weld parts of Torino bodies. There are, of course, possible military applications.

We address ourselves, then, to a detailed examination of what happens when the light interacts with the material. It is convenient to think of this interaction in three parts, although all three influence each other and take place simultaneously.

First, the light couples with the material. To a first approximation, this is governed by simple optical reflectivity, although at high power densities other effects become important. The net result of the coupling is the conversion of some fraction of the optical energy into thermal and/or mechanical energy.

Second, the thermomechanical signal is propagated into the material. The details of this propagation play a prominent role in determining the net effect of the irradiation. For example, pure copper or aluminum, with their high thermal diffusivity, can readily dissipate large amounts of thermal energy and thus require higher intensities for, say, laser welding than more poorly conducting metals like stainless steel.

6

Third is the induced effect, the effect the thermomechanical energy has on the material, such as melting or vaporization, shock loading, crack propagation, and so on. Here again there is an interplay with the other parts. When a metal, for example, begins to melt, its optical reflectivity and thermal diffusivity change markedly, and this changes the coupling and the energy flow. So in our discussion we shall have to be aware of the interaction between the three aspects of coupling, energy flow, and induced effects.

2. OPTICAL REFLECTIVITY

2.1. General Properties

To consider the coupling of the laser energy to a material, we need first to know the optical reflectivity R and the transmissivity T for light incident on a surface which divides two semi-infinite media. The transmissivity plus the reflectivity equals unity *at a single surface*:

$$R + T = 1. \tag{7}$$

In most practical situations we are dealing with more than one surface; typically, we have a slab of material with light impinging on one surface. Some light is reflected, and the rest is either absorbed or passes completely through the slab. In such a situation we shall describe the net result of all the reflection, after multiple passes inside the slab and appropriate absorption has been accounted for, in terms of the reflectance $\mathcal{R}$, the absorptance $\mathcal{A}$, and the transmittance $\mathcal{T}$:

$$\mathcal{R} + \mathcal{T} + \mathcal{A} = 1. \tag{8}$$

What we really are interested in from the point of view of material response is $\mathcal{A}$, the absorptance of the material. In most materials of interest from the practical aim of using lasers to melt, weld, etc., $\mathcal{T}$ is zero, and

$$\mathcal{R} + \mathcal{A} = 1. \tag{9}$$

In a later section we shall consider the relationship between $\mathcal{R}$ and R.

To understand reflectivity, we must use some general results from the theory of electromagnetic waves. Let us summarize these briefly at this point. The electric field of the electromagnetic wave, from Eq. (2), is

$$\mathcal{E} = \text{Re} \left[\mathcal{E}_0 e^{-2\pi k z/\lambda} e^{i\omega(t - nz/c)} \right].$$

The relationships we need are those among the index of refraction n, the extinction coefficient k, and the material properties. These relationships can be derived by substituting Eq. (2) in the wave equation

$$\frac{\partial^2 \mathcal{E}}{\partial z^2} = \mu\epsilon \frac{\partial^2 \mathcal{E}}{\partial t^2} + \mu\sigma \frac{\partial \mathcal{E}}{\partial t}. \tag{10a}$$

This results in the expression

$$\left(\frac{2\pi k}{\lambda} + \frac{i\omega n}{c}\right)^2 = \mu\epsilon(-\omega^2) + i\omega\mu\sigma .$$ (10b)

Note that we are using rationalized MKS units throughout. The material properties enter through μ, ϵ, and σ, which are the magnetic permeability, the dielectric function, and the electric conductivity of the medium. Using the usual equations between the field vectors

$$\mathbf{D} = K_e \epsilon_0 \mathcal{E} ,$$ (11a)

$$\mathbf{B} = K_m \mu_0 \mathbf{H},$$ (11b)

$$\mathbf{J} = \sigma \mathcal{E} ,$$ (11c)

we have

$$\epsilon = K_e \epsilon_0 ,$$ (11d)

$$\mu = K_m \mu_0 .$$ (11e)

In Eqs. (11), ϵ_0 and μ_0 are the electric permittivity and magnetic permeability of a vacuum. K_e is the dielectric constant and K_m the magnetic permeability of the material. By substituting Eqs. (11d) and (11e) into Eq. (10b) and using $2\pi/\lambda = \omega/c$, we obtain

$$(k + in)^2 = -K_e K_m \epsilon_0 \mu_0 c^2 + i K_m \mu_0 \sigma \frac{c^2}{\omega}.$$

Finally, if we introduce $c^2 = (\epsilon_0 \mu_0)^{-1}$ and do some algebra,

$$n - ik = \sqrt{K_m} \sqrt{K_e - i \frac{\sigma}{\epsilon_0 \omega}}.$$ (12)

This equation relates the material parameters K_m, K_e, and σ, which in general may be complex, to index of refraction n and extinction coefficient k. To describe the propagation of the light wave thus requires a knowledge of K_e, K_m, and σ. Before we describe these, let us look at two more general properties of our propagating electromagnetic wave.

The first of these is absorption. If the medium is absorbing, the intensity will fall off to $1/e$ of its initial value in a distance δ, obtained by setting $\mathcal{E}^2$ of Eq. (2) equal to $(1/e)\mathcal{E}_{max}^2$, or

$$\frac{4\pi k \delta}{\lambda} = 1$$

$$\delta = \frac{\lambda}{4\pi k}.$$ (13)

This shows why k is called the extinction coefficient, for it determines skin depth δ. Equation (13) is fairly general in that once k is known, δ can be calculated. As noted, a knowledge of the material properties is required to calculate k.

The second general property we wish to derive is the expression for reflectivity, in terms of n and k. To do this, consider light impinging normally onto an ideal solid surface, as shown in Fig. 4. Here we have illustrated the incident $(\mathscr{E}_i)$, reflected $(\mathscr{E}_r)$, and transmitted $(\mathscr{E}_t)$ electric waves at a vacuum—material interface. For the present, we limit our discussion to the case of normal incidence. We now consider the boundary condition. We have

$$\mathscr{E}_i + \mathscr{E}_r = \mathscr{E}_t \tag{14}$$

for the electric field. For the magnetic field **B**, we write

$$B_i - B_r = B_t . \tag{15}$$
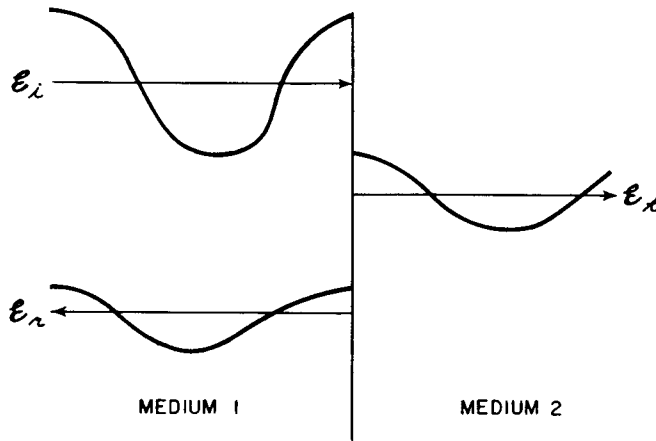
Fig. 4—Incident, transmitted, and reflected electric
vectors at an interface

The minus sign is before B_r because $\mathscr{E} \times \mathbf{B}$ is positive in the direction of propagation of the wave. Now, the relationship between **B** and $\mathscr{E}$, or, since $\mathbf{B} = \mu\mathbf{H}$, between **H** and $\mathscr{E}$, is required in order to proceed further. This follows directly from Maxwell's equations:

$$\nabla \times \mathscr{E} = -\mu \frac{\partial \mathbf{H}}{\partial t} \tag{16}$$

$$\nabla \times \mathbf{H} = \sigma \mathscr{E} + \epsilon \frac{\partial \mathscr{E}}{\partial t}. \tag{17}$$

It is convenient to rewrite Eq. (2) and introduce $\omega\lambda = 2\pi c$, to have $\mathscr{E}$ explicitly in terms of ω instead of both ω and λ. Recall that $\mathscr{E}$ is a vector, and take it as being along the x direction. Thus

$$\mathscr{E}_x = \mathscr{E}_0 e^{i\omega t} e^{-\frac{i\omega}{c} z(n-ik)} . \tag{18}$$

Here we have dropped the "Re" notation, and shall simply note that we always mean the real part when we write the wave in exponential form. We shall use unit vectors $\hat{x}$, $\hat{y}$, and $\hat{z}$.

Now the curl expressions reduce to

$$\nabla \times \mathcal{E} = \hat{y} \frac{\partial \mathcal{E}_x}{\partial z},$$

which, with Eq. (16), tells us that **H** has only a y component, so

$$\nabla \times \mathbf{H} = -\hat{x} \frac{\partial \mathbf{H}_y}{\partial z}.$$

Thus Eqs. (16) and (17) become

$$\frac{\partial \mathcal{E}_x}{\partial z} = -\mu \frac{\partial H_y}{\partial t} \tag{19}$$

and

$$-\frac{\partial H_y}{\partial z} = \sigma \mathcal{E}_x + \epsilon \frac{\partial \mathcal{E}_x}{\partial t} \tag{20}$$

and, of course, $\mathcal{E}_y = \mathcal{E}_z = H_x = H_z = 0$. Putting the expression for $\mathcal{E}_x$ from Eq. (18) into Eq. (19) leads to

$$H_y = \frac{n - ik}{\mu c} \mathcal{E}_0 e^{-\frac{i\omega}{c} z(n - ik)} e^{i\omega t}.$$

This is the desired relationship:

$$H_y = \left(\frac{n - ik}{\mu c}\right) \mathcal{E}_x. \tag{21}$$

At this point we note in passing that Eq. (20) or (10b) could be used to yield the relationship of n and k to μ, ϵ, and σ. If the reader is unfamiliar with these relationships, it is instructive to carry out the algebra.

Returning to our consideration of the reflected electric and magnetic fields, we rewrite Eqs. (14) and (15) with the help of the relationship between H and $\mathcal{E}$, from Eq. (21);

$$\mathcal{E}_i + \mathcal{E}_r = \mathcal{E}_t$$

and

$$\mu_1 H_1 - \mu_1 H_r = \mu_2 H_t$$

becomes

$$\mathscr{E}_i - \mathscr{E}_r = \left(\frac{n_2 - ik_2}{n_2 - ik_1}\right) \mathscr{E}_t.$$

Solve for $\mathscr{E}_r/\mathscr{E}_i$ by eliminating $\mathscr{E}_t$:

$$\frac{\mathscr{E}_r}{\mathscr{E}_i} = \frac{n_1 - n_2 - i(k_1 - k_2)}{n_1 + n_2 - i(k_1 + k_2)}.$$

Finally, the reflectivity R at the surface is

$$R = \left|\frac{\mathscr{E}_r}{\mathscr{E}_i}\right|^2 = \frac{(n_1 - n_2)^2 + (k_1 - k_2)^2}{(n_1 + n_2)^2 + (k_1 + k_2)^2}. \tag{22}$$

Take medium 1 as a vacuum and drop the subscript 2. This gives, since in a vacuum $n_1 = 1$ and $k_1 = 0$,

$$R = \frac{(n - 1)^2 + k^2}{(n + 1)^2 + k^2}. \tag{23}$$

Equation (23) is the second relationship we will find useful in discussing the coupling of optical radiation with metals. Note that it is derived for the special case of normal incidence and is applicable to a vacuum-material interface.

2.2. Reflectivity of Metals at Infrared Wavelengths

We turn now to a derivation of the optical reflectivity of metals for infrared wavelengths, where experiment has shown that the free-electron theory (sometimes called the Drude-Lorentz theory) of metals is adequate. This theory rests on three assumptions. The first is that electromagnetic radiation interacts only with the free electrons in the metal. The second is that the free electrons obey Ohm's law, or, more specifically, that

$$m^* \frac{dv}{dt} + \frac{m^*}{\tau} v = -e\mathscr{E} \tag{24}$$

where m^* is the effective mass of the electron, v the velocity, τ the relaxation time due to collisions, and $-e\mathscr{E}$ the force on the electron due to the electromagnetic field. The third assumption is that the free electrons of a metal can be described in terms of a single effective mass, carrier concentration, and relaxation time. There has been a good deal of discussion about the validity of these assumptions in the literature. Recent work [3] indicates that, for wavelengths in the intermediate infrared (a few microns to many tens of microns) and beyond, the free-electron theory does a reasonable job of predicting the reflectivity of metals.

To derive the free-electron optical reflectivity, we try solutions to Eq. (24) of the form

$$v \approx e^{i\omega t},$$

11

so that

$$\left[m^*(i\omega) + \frac{m^*}{\tau} \right] v = -e\mathcal{E}$$

and

$$v = -\frac{e\tau}{m^*(1 + i\omega\tau)} \mathcal{E} .$$

Now the current flow obeys

$$\mathbf{J} = \sigma\mathcal{E} = -Nev$$

where N is the electron concentration (number of electrons per unit volume). By comparison of the last two equations,

$$\frac{\sigma}{Ne} = \frac{e\tau}{m^*(1 + i\omega\tau)}$$

or

$$\sigma = \frac{Ne^2\tau}{m^*(1 + i\omega\tau)} .$$

Now the dc conductivity is

$$\sigma_0 = \frac{Ne^2\tau}{m^*} . \tag{25a}$$

We see σ is a complex quantity and seek to write it as the sum of a real and imaginary part. Thus,

$$\sigma = \frac{Ne^2\tau(1 - i\omega\tau)}{m^*(1 + \omega^2\tau^2)} .$$

Define

$$\sigma = \sigma_1 - i\sigma_2 .$$

The result is

$$\sigma_1 = \frac{\sigma_0}{1 + \omega^2\tau^2} \tag{25b}$$

$$\sigma_2 = \frac{\sigma_0\omega\tau}{1 + \omega^2\tau^2} . \tag{25c}$$

To proceed further we need to use the general expression for electromagnetic waves developed in Sec. 2.1. Recall Eq. (12):

$$n - ik = \sqrt{K_m} \sqrt{K_e - i \frac{\sigma}{\epsilon_0 \omega}}$$

and, from the complex σ,

$$n - ik = \sqrt{K_m} \sqrt{K_e - i \frac{\sigma_1 - i\sigma_2}{\epsilon_0 \omega}}.$$

If we assume only free-electron optical interactions, the metal does not polarize under the wave, and $K_e = 1$. In addition, for metals in the infrared, $K_m = 1$. Thus,

$$n - ik = \sqrt{1 - \frac{i\sigma_1 + \sigma_2}{\epsilon_0 \omega}}$$

or

$$n - ik = \sqrt{1 - \frac{\sigma_2}{\epsilon_0 \omega} - i \frac{\sigma_1}{\epsilon_0 \omega}}. \tag{26}$$

It remains only to separate the real and imaginary parts of Eq. (26), which will yield two equations in n and k and thus give n and k in terms of the dc conductivity σ_0 and the relaxation time τ. Then we can use our expression for the reflectivity from Eq. (23) to generate R from n and k.

To carry out the algebra we use the identity

$$\sqrt{A + iB} = \sqrt{\frac{R + A}{2}} + i \sqrt{\frac{R - A}{2}}$$

where

$$R = \sqrt{A^2 + B^2}.$$

Letting

$$A = 1 - \frac{\sigma_2}{\epsilon_0 \omega}$$

and

$$B = - \frac{\sigma_1}{\epsilon_0 \omega},$$

we have

$$2n^2 = \left(i - \frac{\sigma_2}{\epsilon_0 \omega}\right) + \sqrt{\left(1 - \frac{\sigma_2}{\epsilon_0 \omega}\right)^2 + \left(\frac{\sigma_1}{\epsilon_0 \omega}\right)^2} \tag{27a}$$

and

$$2k^2 = -\left(1 - \frac{\sigma_2}{\epsilon_0 \omega}\right) + \sqrt{\left(1 - \frac{\sigma_2}{\epsilon_0 \omega}\right)^2 + \left(\frac{\sigma_1}{\epsilon_0 \omega}\right)^2}. \tag{27b}$$

Equations (27a) and (27b), together with

$$R = \frac{(n-1)^2 + k^2}{(n+1)^2 + k^2}$$

(Eq. (23)), give the reflectivity. These are elaborate expressions indeed. It is useful to look at some limiting cases and at the material parameters that determine R.

Notice that R is a function solely of σ_1, σ_2, and ω. Look again at Eqs. (25) and note that σ_0 can be used to replace τ in the expression for σ_1 and σ_2:

$$\sigma_1 = \frac{\sigma_0}{1 + \omega^2 \dfrac{m^{*2}\sigma_0^2}{N^2 e^4}} \tag{28a}$$

$$\sigma_2 = \frac{\sigma_0^2 \dfrac{m^*}{N e^2} \omega}{1 + \omega^2 \dfrac{m^{*2}\sigma_0^2}{N^2 e^4}}. \tag{28b}$$

Equations (28) show that σ_1 and σ_2, and thus R, depend on frequency ω, constant m^*/N, and dc conductivity σ_0. Thus

$$R = f(\omega, \sigma_0, m^*/N). \tag{29}$$

This means that we can use the dc conductivity to predict the reflectivity. Furthermore, if we know the temperature variation of σ_0, we can use this method to calculate R as a function of temperature. This is a useful result, because it is difficult to measure optical reflectivity as a function of temperature, whereas it is fairly easy to measure σ_0 vs temperature. A wealth of data on electrical conductivity has been amassed for most metals and alloys. Thus the free-electron model is currently enjoying a great deal of attention as a way of providing reflectivity-vs-temperature information in the study of laser effects.

There is, of course, one problem in using $\sigma_0(T)$ data to predict R, and that is the parameter m^*/N. It turns out that R is fairly insensitive to this parameter at infrared wavelengths. To see this we show here some numerical illustration. Define

$$\beta = m^*/m_0$$

where m_0 is the free electron mass, and then the parameter β/N is equivalent to m^*/N. Figure 5 shows a plot of $\partial R/\partial(\beta/N)$ as a function of β/N for $\lambda = 10~\mu$m and various values of σ_0. Here σ_0 is in units of reciprocal ohm-centimeters. Typical values are, for example,

$\sigma_0 = 10^5 \; \Omega^{-1} \; cm^{-1}$ and $\beta/N = 10^{-23} \; cm^3$ for aluminum. Then the value of $\partial R/\partial(\beta/N)$ is about $7.2 \times 10^{20} \; cm^{-3}$. If we take a 10% error in β/N we get

$$\frac{\partial R}{\partial(\beta/N)} \; \Delta(\beta/N) \; = \; 7.2 \times 10^{20} \times 10^{-24}$$

$$\Delta R \; = \; 0.00072 \, .$$

Since for these values $R = 0.97366$, the change in R is only about 0.1%. We can obtain quite good predictions by the Drude-Lorentz model using the experimental values of σ_0 and the most simple choice for β/N, namely one free electron for each valence electron per atom in the metal, and $\beta = 1$. For alloys, it is sufficient to choose the major constituent of the alloy. For example, with stainless steel we choose iron, or two electrons per atom, to compute N and hence β/N.
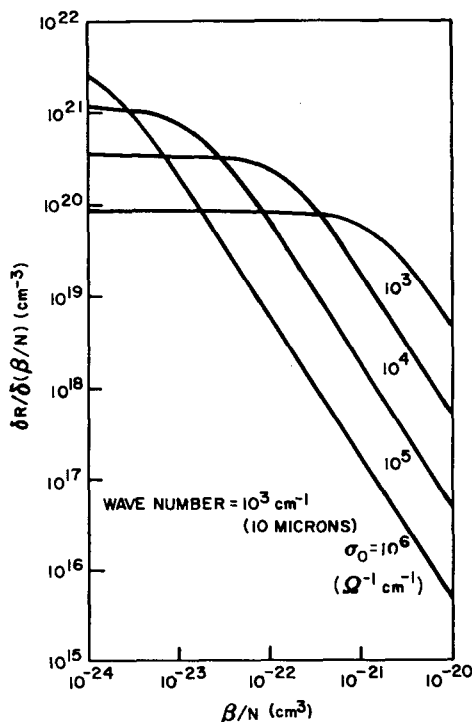
Fig. 5—Sensitivity of R to the parameter
β/N (Ref. 3)

Figures 6 and 7 show the predictions of the free-electron theory for a variety of metals and some comparison to experimental data [3]. The abrupt change when the metal melts is caused by the abrupt change in the dc conductivity. Notice in the comparison to data that aluminum films give values closest to the theory. This is probably because they present the best surfaces. Defects, oxide layers, etc., tend to trap the incident radiation and cause the real surface to absorb more radiation than the ideal surface. These graphs are in terms of absorptance, which is the experimentally measured quantity, and, since metals are opaque, $\mathcal{Q} = 1 - \mathcal{R}$, which is correct for specular reflection at normal incidence from an opaque substance.
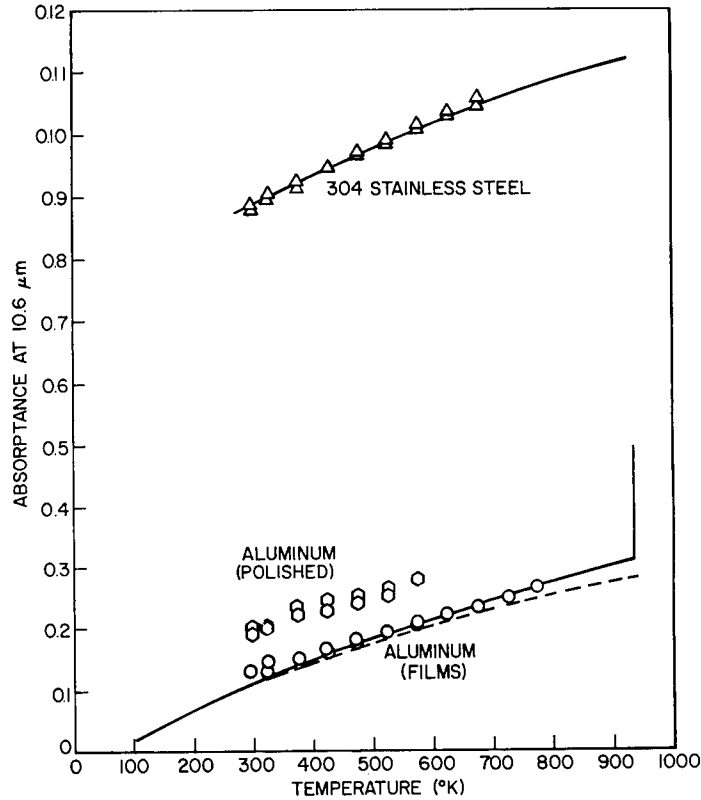
Fig. 6—Temperature dependence of the absorptance at 10.6 μ
for aluminum and stainless steel

Let us return to the expressions for n and k to look at some limiting forms and thus show how these complete expressions reduce to simple relationships. Remember that R (Eq. (23) is determined by n and k (Eqs. (27), which are in turn obtained from the dc conductivity and m^*/N (Eqs. (28). The variation of n and k with wavelength is shown in Fig. 8 for a typical good conductor like aluminum or copper at room temperature. Note that at long wavelengths $n = k$. We can derive this by using Eqs. (25) for σ_1 and σ_2 and noting that as $\omega \rightarrow o$, $\sigma_1 \rightarrow \sigma_0$, and $\sigma_2 \rightarrow \sigma_0 \omega \tau$. By substituting these into Eqs. (27) for n and k, we can readily show that

$$n = k = \sqrt{\frac{\sigma_0}{2\epsilon_0 \omega}}. \qquad (30)$$

This is called the Hagen-Rubens limit. Note that n is very large. Under these conditions algebra can be used to reduce Eq. (23) to

$$R = \frac{n-1}{n+1}$$

or

$$R = 1 - \frac{2}{n},$$

16
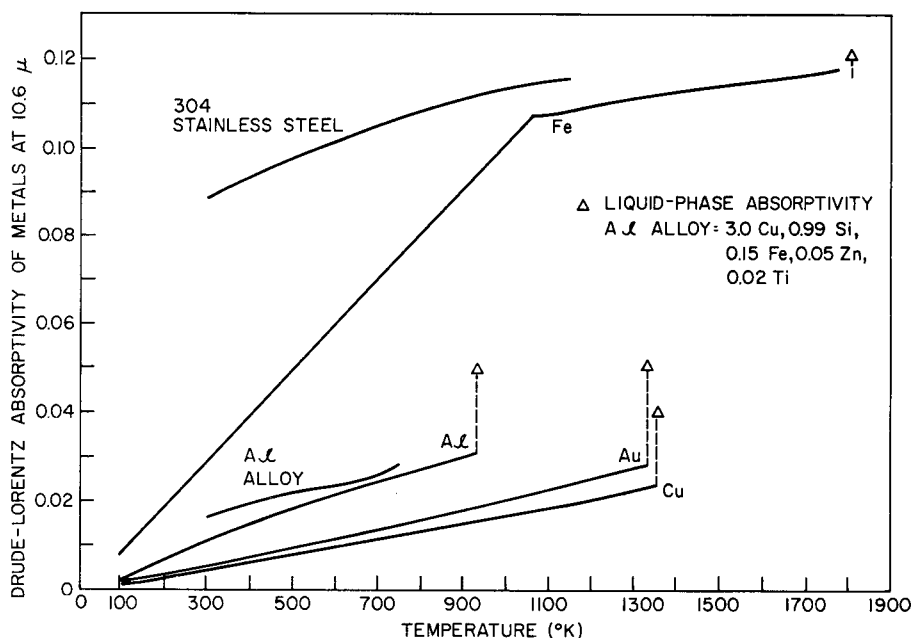
Fig. 7—Free electron theory predictions of absorptivity of several metals at 10.6 μ. The open symbols indicate the molten state.
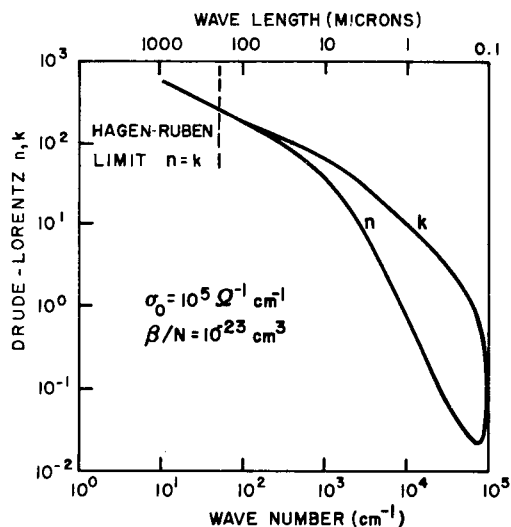

Fig. 8—n and k as functions of wavelength (Ref. 3)

17

and Eq. (30) can be substituted for n to get

$$R = 1 - 2 \sqrt{\frac{2\omega\epsilon_0}{\sigma_0}} . \tag{31}$$

This is the Hagen-Rubens reflectivity.

We can also comment on the skin depth. We have, at long wavelengths ($\omega \to o$),

$$\delta = \frac{\lambda}{2\pi} \sqrt{\frac{2\epsilon_0\omega}{\sigma_0}} .$$

This can be rewritten as

$$\delta = \sqrt{\frac{2}{\mu_0\sigma_0\omega}} . \tag{32}$$

Equation (32) is the common expression for skin depth used at long wavelengths.

Finally, we see from Fig. 9 that n and k reconverge at short wavelengths. This is called the plasma resonance. To see this, one must look at the behavior of n and k over a larger spectrum. We have already discussed the long-wavelength limiting behavior of n and k. This is the Hagen-Rubens region, where $n = k$. At short wavelengths, it is easy to show from Eqs. (28) that

$$\sigma_1 \to \frac{N^2 e^4}{m^{*2}\sigma_0\omega^2}$$

$$\sigma_2 \to \frac{Ne^2}{m^*\omega} .$$
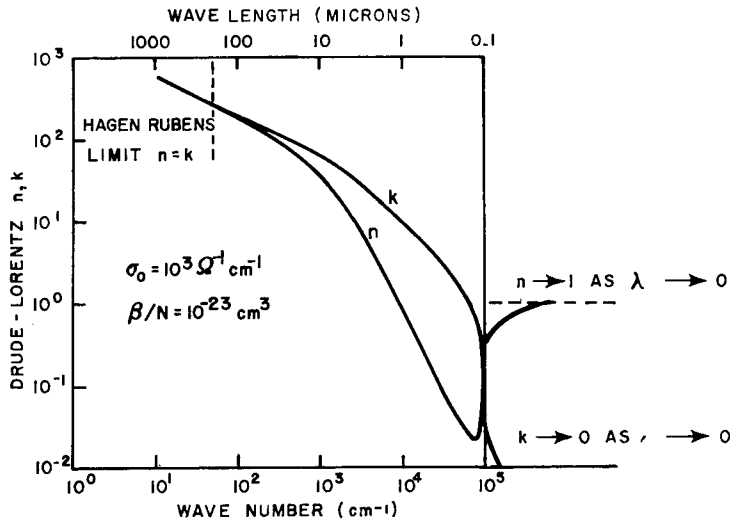
Fig. 9—n and k as functions of wavelength

Thus Eq. (27) can be written, for large ω, as

$$n^2 = 1 - \frac{Ne^2}{\epsilon_0 m^* \omega^2} \tag{33a}$$

$$k^2 = 0. \tag{33b}$$

Now the plasma frequency is usually defined from Eq. (33a) by setting $n = 0$ to yield

$$\omega_p^2 = \frac{Ne^2}{\epsilon_0 m^*} \tag{34a}$$

and thus

$$n^2 = 1 - \frac{\omega_p^2}{\omega^2}. \tag{34b}$$

We see, then, that at very high frequencies the free-electron model predicts a transparent behavior ($k = 0$) and the index of refraction approaches that of a vacuum. The transition to this transparent behavior takes place at the plasma frequency, and it is a fairly abrupt transition, as Fig. 9 shows. In fact, some texts call this transition the "ultraviolet catastrophe." Note that at ω near ω_p Eqs. (34) and (33) are not valid. For these frequencies we must use the full expression. If we use again the values of $\sigma_0 = 10^5 \ \Omega^{-1}\text{cm}^{-1}$ and $\beta/N = 10^{-23} \ \text{cm}^3$, which are appropriate to a good conductor like aluminum at room temperature, the reflectivity looks like Fig. 10. One can see that, in terms of the reflectivity, the transition is very abrupt, indeed.
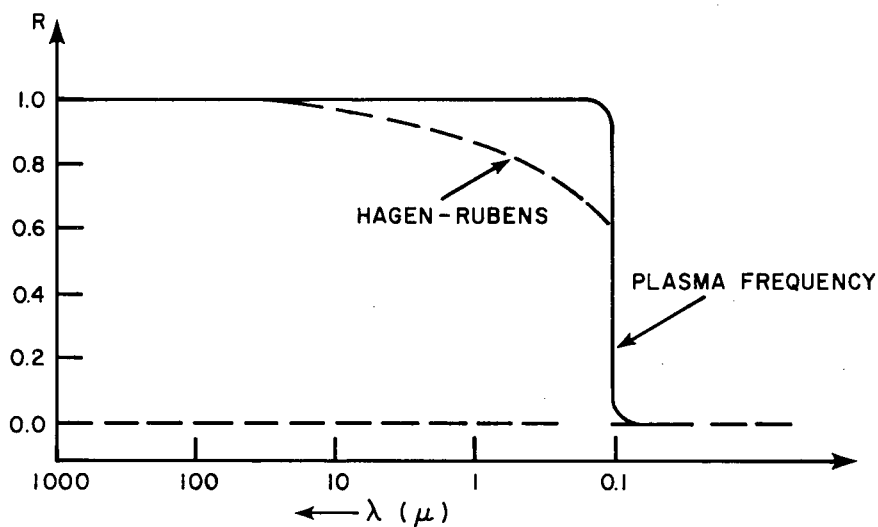

Fig. 10—R as a function of wavelength

The optical reflectivity of real metals is, as we have seen, in reasonable accord with the free-electron model at wavelengths in the infrared. The surface, however, must be nearly perfect for the predicted reflectivities to be achieved, and, of course, as the wavelengths approach the visible region band effects become important and the reflectivity shows rapid fluctuations with frequency. The absorptance of a practical metal surface is still largely an empirical matter. For high-power, continuous-wave radiation by a CO_2 laser, some data are available, but very little information on absorptivity as a function of surface temperature under these conditions is available. Shown in Table 1 are room-temperature absorptances for a few materials.

Table 1
Room-Temperature Absorbtances of Aerospace
Metals and Alloys at 10.6 μm for Various Surface
Conditions and at Normal Incidence

Metal or Alloy	Surface Condition			
	Ideal	Polished	As-Received	Sandblasted
Al	0.013	0.030	0.04 ±0.02	0.115 ±0.015
Au	0.006	0.01	0.02	0.14
Cu	0.011	0.016		0.06
Ag	0.005	0.011		
2024 Al		0.033	0.07 ±0.02	0.25
304 Stainless steel		0.11	0.4 ±0.2	
Ti Alloy (6Al, 4V)			0.65 ±0.2	
Mg Alloy Az-31B			0.06 ±0.03	

Data on the reflectivity of a metal during actual irradiation by a laser beam is quite difficult to obtain, although this information is central to the problem of laser-material interaction. One classic experiment along these lines was carried out by Bonch-Bruevich, Imas, Romanov, Libenson, and Mal'tsev in *Russia in 1967* [4]. They surrounded their specimens with a sphere to monitor the reflected radiation, as shown schematically in Fig. 11. The output of the photodetector is proportional to the reflectance of the specimen. Some of their results for steel and copper are shown in Fig. 12. The laser pulse (Nd: glass laser, 1.06 μm), with a peak power density of the order of 10^8 W/cm^2, is shown as a broken line. As time passes, of course, the laser pulse heats the surface and the reflectance decreases. An especially interesting feature of these data is the shoulder. The author has suggested that this leveling off is associated with the surface reaching the melting point and pausing at that temperature while the thickness of the molten layer
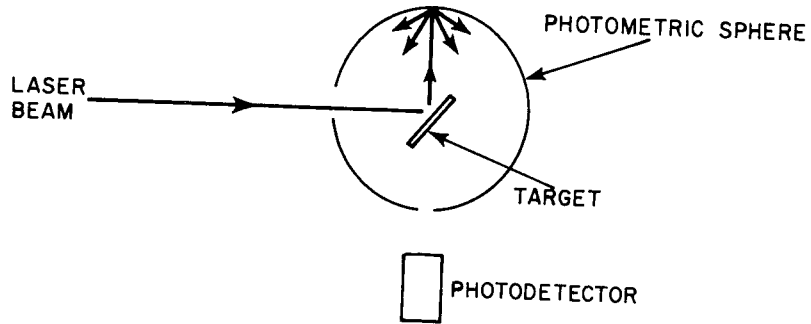
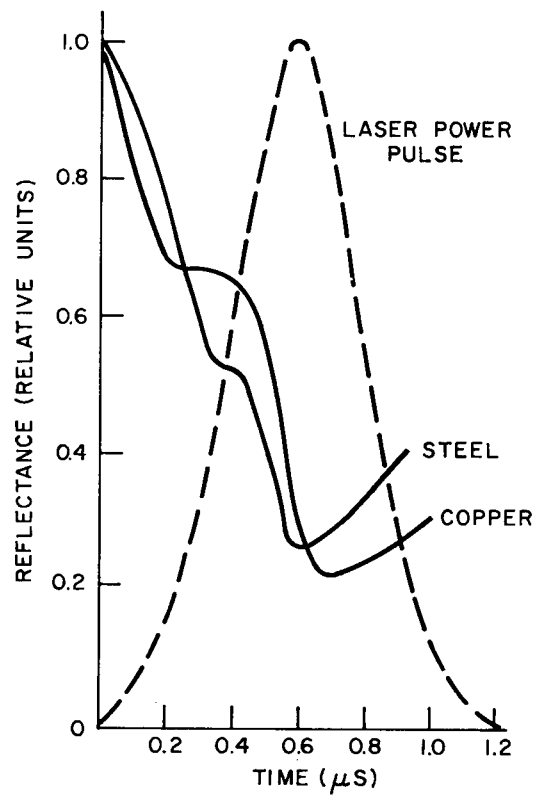Fig. 11—Schematic representation of Bonch-Bruevich experiment

Fig. 12—Reflectance of steel and copper during irradiation by a laser beam (from Ref. 5; copyright 1969, Clarendon Press, Oxford, England. Used by permission of J.C. Jaeger).

propagates into the solid. In short order, however, the molten layer begins to heat up and the reflectance continues to decrease. As the power density of the laser pulse reaches its peak and begins to fall, the surface temperature can no longer be maintained, and as the surface cools the reflectance begins to increase again.

3. THERMAL RESPONSE

3.1. Introduction

One of the most important effects of intense laser irradiation is the conversion of the optical energy in the beam into thermal energy in the material. This is the basis of many applications of lasers, such as welding and cutting. We shall summarize here this thermal response. It is basically a classical problem, namely heat flow. In the usual manner, we shall seek solutions to the equation which governs the flow of heat, namely

$$\rho C \, \frac{\partial T}{\partial t} = \frac{\partial}{\partial x} \, K\!\left(\frac{\partial T}{\partial x}\right) + \frac{\partial}{\partial y} \, \left(K \, \frac{\partial T}{\partial y}\right) + \frac{\partial}{\partial z} \, \left(K \, \frac{\partial T}{\partial z}\right) + A \, . \tag{35}$$

We use here ρ for the density, C for the specific heat, T for temperature, t for time, and K for thermal conductivity. A is the heat produced per unit volume per unit of time. In Eq. (35), ρ, C, and K are considered functions of both position and temperature, and A is a function of both position and time. In effect, the equation is a simple statement that the rate at which heat accumulates in an elemental volume $dxdydz$ is equal to the net flow of heat across the faces of that volume plus the rate at which heat is produced within the volume.

Thus thermal response studies consist essentially of two parts. First, one needs to know the rate and source of production of heat by the laser, which yields A. Then one solves Eq. (35) subject to the boundary conditions of the situation of interest. This can be a very elaborate task and frequently can be done only with the aid of a computer. There is a great deal of effort among workers in the field of laser effects to develop an all-inclusive computer program to solve Eq. (35) for every possible situation. However, the solution to Eq. (35) can be no better than the knowledge of A, and, as we shall see in later sections, it is often very difficult to establish A with any precision in a laser—material interaction situation.

3.2. No Phase Change—Semi-Infinite Solid

Let us consider first the most simple situation. Let the laser beam be perfectly uniform over an extremely large area, so that we have a one-dimensional situation. Assume also that the material parameters are temperature-independent and that the solid is uniform and isotropic and of semi-infinite extent (Fig. 13). Finally, assume that there is no phase change; the rate at which energy enters the material is not sufficient to induce melting or vaporization.

First rewrite Eq. (35), using the fact that ρ, C, and K are constant:

$$\frac{\partial^2 T}{\partial z^2} - \frac{1}{\kappa} \, \frac{\partial T}{\partial t} = -\frac{A}{K}. \tag{36}$$
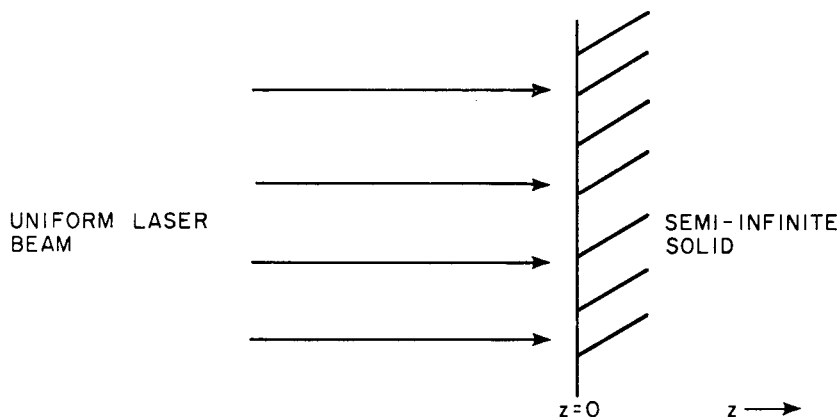
Fig. 13—Uniform irradiation of a semi-infinite solid

Here we have introduced $\kappa = K/(\rho C)$, which is the thermal diffusivity. Let us adopt the convention that T is measured with respect to the initial (or ambient) temperature of the material. This is possible because Eqs. (35) and (36) define T only to within an additive constant. Then we have as a boundary condition that $T \rightarrow 0$ as $z \rightarrow \infty$. The boundary condition on the front face ($z = 0$) depends on what we assume for radiative and convective losses. It can be shown that, for most cases of interest, the rate at which the laser creates heat at the interface is overwhelmingly larger than convective and radiation losses, so we ignore them for the present calculation. Thus the boundary condition is that there is no heat flux at $z = 0$, that is,

$$K \left. \frac{\partial T}{\partial z} \right)_{z=0} = 0 .$$

Now consider A. Denote by I the power density of the laser radiation at the surface; the dimensions of I are power per unit area. The power density of the radiation transmitted to the surface is $I(1 - \mathscr{R})$. Then the power density as a function of z is

$$F = (1 - \mathscr{R}) I \, e^{-4\pi k z/\lambda} . \tag{37}$$

This follows from the fact that the energy in the electromagnetic wave goes as $\mathscr{E}^2$. Now to get the power transferred per unit volume, consider elemental volumes of length dz and unit area:

$$A = -\frac{\partial F}{\partial z} = (1 - \mathscr{R}) I \, \frac{4\pi k}{\lambda} \, e^{-4\pi k z/\lambda} . \tag{38}$$

The minus sign appears because $\partial F/\partial z$ is the power per unit volume lost by the radiation and A is the power per unit volume absorbed by the material. Finally, we define the absorption coefficient

$$\alpha = \frac{4\pi k}{\lambda} , \tag{39}$$

23

which is, of course, $1/\delta$, the skin depth. Thus

$$A(z, t) = (1 - \mathcal{R})I(t)\alpha\, e^{-\alpha z} \tag{40}$$

where we have included the possibility of I varying with time.

So the equation to be solved is

$$\frac{\partial^2 T}{\partial z^2} - \frac{1}{\kappa}\frac{\partial T}{\partial t} = -\frac{(1 - \mathcal{R})I(t)\alpha\, e^{-\alpha z}}{K}. \tag{41}$$

In keeping with our assumption of temperature-independent thermal parameters, we assume further that R is independent of temperature. Equation (40) is valid for temperature-dependent $\mathcal{R}$ and can be used to give $A(z, t, T)$.

For metals, α is a fairly large number. As we saw in Sec. 2, k is of the order of 100 at $\lambda = 10$ μm, so that α is of the order of 10^6 cm^{-1}. Hence the absorption occurs in a very narrow layer at the surface. It then becomes more convenient to seek solutions of

$$\frac{\partial^2 T}{\partial z^2} - \frac{1}{\kappa}\frac{\partial T}{\partial t} = 0 \tag{42}$$

subject to the boundary conditions that $T = 0$ at $z = \infty$, but with a specified flux into the surface at $z = 0$, i.e.,

$$-K\left.\frac{\partial T}{\partial z}\right)_{z=0} = (1 - \mathcal{R})I(t)$$

or, with the definition

$$F(t) = (1 - \mathcal{R})I(t), \tag{43}$$

$$-K\left.\frac{\partial T}{\partial z}\right)_{z=0} = F(t). \tag{44}$$

First examine the case of $F = F_0$, a constant. This is appropriate to irradiation by a continuous laser, given temperature-independent material properties. We note here only the solution, for many excellent texts on heat conduction can be consulted for the details [5].

The solution to this problem is

$$T(z, t) = \frac{2F_0\sqrt{\kappa t}}{K}\,\text{ierfc}\,[z/(2\sqrt{\kappa t})] \tag{45}$$

or

$$T(z, t) = \frac{2F_0}{K}\left\{\sqrt{\frac{\kappa t}{\pi}}\,e^{-z^2/4\kappa t} - \frac{z}{2}\,\text{erfc}\,[z/(2\sqrt{\kappa t})]\right\}.$$

The functions which appear here are error functions, and it is useful to summarize some of their properties and definitions. (See Ref. 5, Ch. II.)

The error function is

$$\text{erf}(x) = \frac{2}{\sqrt{\pi}} \int_0^x e^{-\ell^2} d\ell$$

$$\text{erf}(o) = 0, \quad \text{erf}(\infty) = 1, \quad \text{erf}(-x) = -\text{erf}(x).$$

The complementary error function is

$$\text{erfc}(x) = 1 - \text{erf}(x) = \frac{2}{\sqrt{\pi}} \int_x^\infty e^{-\ell^2} d\ell.$$

The integral of the complementary error function is

$$\text{ierfc}(x) = \int_x^\infty \text{erfc}(\ell) \, d\ell$$

or

$$\text{ierfc}(x) = \frac{1}{\sqrt{\pi}} e^{-x^2} - x \, \text{erfc}(x)$$

$$\text{ierfc}(x) = \frac{1}{\sqrt{\pi}} e^{-x^2} - x + x \, \text{erf}(x).$$

Some derivatives are useful:

$$\frac{\partial \, \text{erf}(x)}{\partial x} = -\frac{\partial \, \text{erfc}(x)}{\partial x} = \frac{2}{\sqrt{\pi}} e^{-x^2}$$

$$\frac{\partial^2 \, \text{erf}(x)}{\partial x^2} = -\frac{\partial^2 \, \text{erfc}(x)}{\partial x^2} = -\frac{4}{\sqrt{\pi}} x \, e^{-x^2}$$

$$\frac{\partial \, \text{ierfc}(x)}{\partial x} = -\text{erfc}(x)$$

$$\frac{\partial^2 \, \text{ierfc}(x)}{\partial x^2} = \frac{2}{\sqrt{\pi}} e^{-x^2}$$

Now we can show that the boundary condition is satisfied. Using the first form of Eq. (45) yields

$$\frac{\partial T}{\partial z} = \frac{2F_0 \sqrt{\kappa t}}{K} \left\{ -\text{erfc}\left[z \big/ \left(2\sqrt{\kappa t}\right)\right] \right\} \frac{1}{2\sqrt{\kappa t}}$$

and since erfc $(o) = 1$,

$$\frac{\partial T}{\partial z}\bigg)_{z=0} = -\frac{F_0}{K}.$$

One can also show that Eq. (45) satisfies Eq. (42).

We can use Eq. (45) to show what the front surface temperature behavior is, under constant irradiation, by setting $z = 0$ so that

$$T(o, t) = \frac{2F_0}{K} \sqrt{\frac{\kappa t}{\pi}}. \tag{46}$$

As an illustration, let us calculate the time required to raise aluminum to its melting point for a power density of 5 kW/cm^2:

$K = 2.3$ W/cm^2

$\kappa \approx 0.9$ cm^2/s

$T_{\text{melt}} \approx 600°C$

$T = T_{\text{melt}} - T_{\text{room}} \approx 600°C$

$F_0 = (1 - \Re)I$

$(1 - \Re) = 0.04$

$F_0 = 0.04 \times 5 \times 10^3 = 200$ W/cm^2.

Then $t = (\pi K^2 T^2)/(4F_0^2 \kappa)$ yields $t \approx 42$ s. In practice, it is very difficult to melt extremely thick slabs of aluminum with even a high-power laser, as these calculations suggest.

Equation (45), although derived for a very simple case, describes many very important features of thermal response to lasers. First we shall define the diffusion length, which is useful in that it permits a wide variety of order-of-magnitude calculations to be made. The thermal diffusion length D is defined as

$$D = 2\sqrt{\kappa t}. \tag{47}$$

Strictly speaking, the thermal diffusion length is defined as the distance required for the temperature to drop to $1/e$ of its initial value and depends somewhat on the geometry and the boundary condition. For most purposes it is sufficient simply to take it as defined by Eq. (47). Looking at our solution (Eq. (45)), for example, we see that

$$T(D, t) = \frac{2F_0}{K} \left\{ \sqrt{\frac{\kappa t}{\pi}} \frac{1}{e} - \frac{D}{2} \text{ erfc } (1) \right\}$$

$$T(D, t) = \frac{2F_0}{K} \left\{ \sqrt{\frac{\kappa t}{\pi}} \frac{1}{e} - \frac{D}{2} (0.1573) \right\}.$$

From Eq. (46),

$$T(D, t) = T(o, t) \left\{ \frac{1}{e} - 0.1573 \sqrt{\pi} \right\}.$$

Thus

$$T(D, t) \approx 0.09 \, T(o, t) \tag{48}$$

in this case, whereas $(1/e) \, T(o, t) \approx 0.37 \, T(o, t)$. Referring to our example of irradiating aluminum for 42 s to reach the melting point, we note that the diffusion length at that time is given by

$$D = 2\sqrt{0.9 \times 42} \approx 12 \, \text{cm} ,$$

and, by Eq. (48), the temperature at distance D into the material is 0.09×600, or about $50°C$ above ambient.

Now let us illustrate the solution (Eq. (45)) graphically (Fig. 14). For convenience rewrite the equation by introducing $D = 2\sqrt{\kappa t}$ and by reducing it to the error function erf, so that

$$T(z, t) = \frac{2F_0}{K} \left[\frac{D}{2\sqrt{\pi}} \cdot e^{-z^2/D^2} - \frac{z}{2} + \frac{z}{2} \, \text{erf} \, (z/D) \right].$$
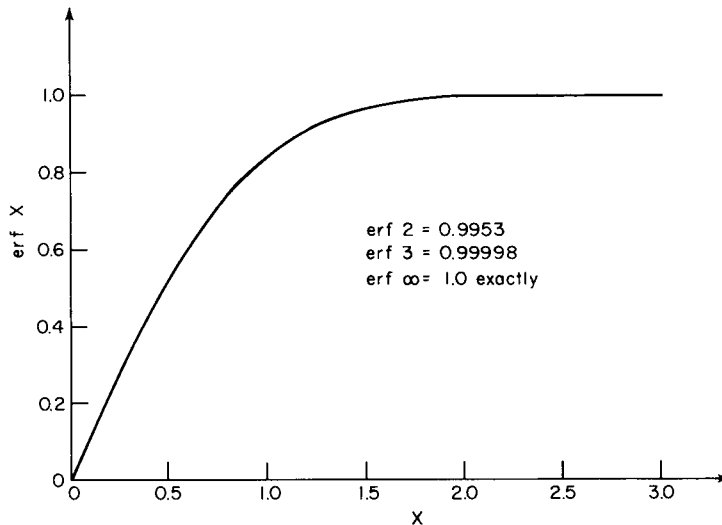

erf 2 = 0.9953
erf 3 = 0.99998
erf ∞= 1.0 exactly

Fig. 14—The error function

Now let $\eta = z/D$, and

$$T(z, t) = \frac{F_0 D}{K}\left[\frac{e^{-\eta^2}}{\sqrt{\pi}} - \eta + \eta \operatorname{erf}(\eta)\right] \tag{49a}$$

or, equivalently in terms of ierfc,

$$T(z, t) = \frac{F_0 D}{K} \operatorname{ierfc}(\eta). \tag{49b}$$

Finally, we define a dimensionless temperature $\theta = TK/(F_0 D)$, so that

$$\theta = \operatorname{ierfc}(\eta). \tag{49c}$$

Thus the plot of the integral of the complementary error function here is the graph of the solution to the problem of constant heat flux on the surface of a semi-infinite solid.

Now, although the graph of Eq. (49c) (see Fig. 15) represents very succinctly the solution to our problem, it does not really show how the temperature varies as a function of position and time. For this purpose it is useful to look at the temperature profiles for various times and see how the profile changes with time. These curves can be generated quickly from $\theta = \operatorname{ierfc}(\eta)$ by recalling the definitions of θ and η and writing them in the following form:

$$T = \left(\frac{2 F_0 \sqrt{\kappa}}{K}\right)\sqrt{t}\, \theta \tag{50a}$$

$$z = 2\sqrt{\kappa}\,\sqrt{t}\,\eta. \tag{50b}$$

ierfc (0) = 0.5642
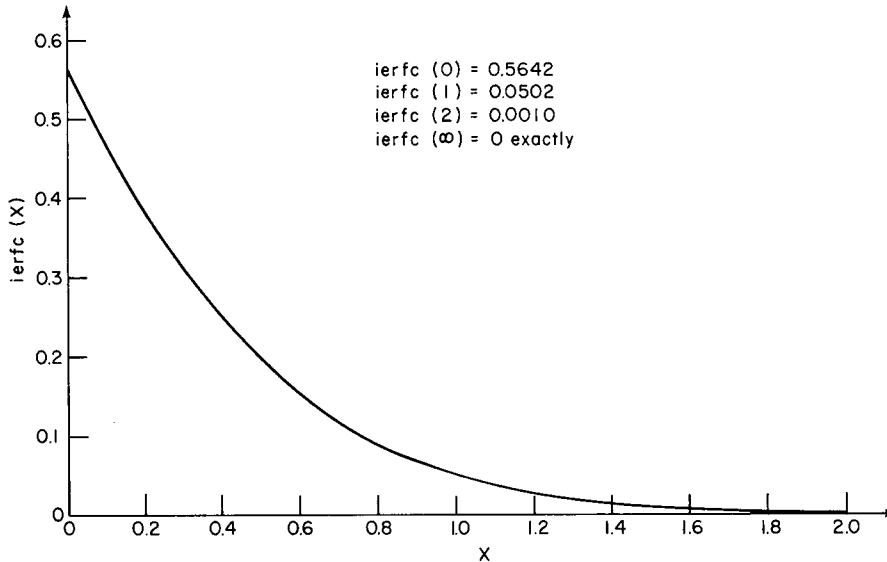ierfc (1) = 0.0502
ierfc (2) = 0.0010
ierfc (∞) = 0 exactly

Fig. 15—The integral of the complimentary error function

28

Thus, at a given time the θ = ierfc (η) curve scales according to Eqs. (50); the basic shape of the curve is unchanged, but it is stretched one way or the other depending on the parameters, and this stretching progresses in time as $\sqrt{t}$. The case of aluminum is shown in Fig. 16.
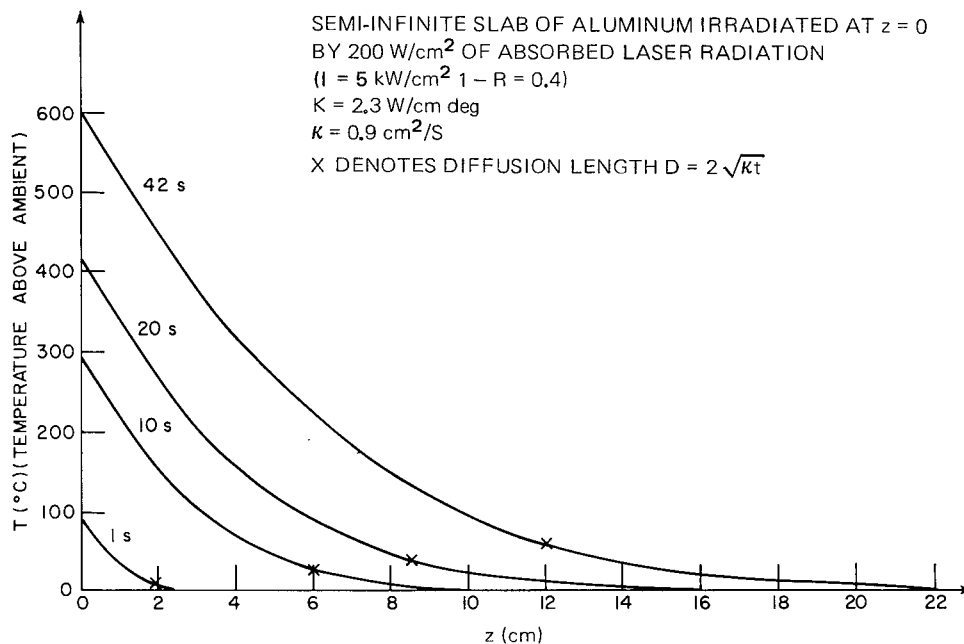

Fig. 16—Laser-induced temperature rise in aluminum as a function of depth

We can also look at the variation of temperature with time at a fixed position. The variation of the surface ($z = 0$) is simply $T(o, t) \approx \sqrt{t}$, as Eq. (46) shows. Wherever $z/(2\sqrt{\kappa t})$ is very small, the temperature variation will approach $\sqrt{t}$. Thus, at any position $T \approx \sqrt{t}$ at sufficiently large t. The temperature-vs-time profiles at fixed position for times such that $z/(2\sqrt{\kappa t})$ is not small can be calculated, of course, from Eq. (45). Some results for aluminum, with the parameters used above, are shown in Fig. 17. Notice that at $z = 10$ cm the temperature profile is far from the "long-time," or $\sqrt{t}$, behavior even at 40 or 50 s, whereas the surface has already begun to melt.

We now turn to some order-of-magnitude arguments. One such argument can be used to estimate the power—pulse length combination which might be expected to yield surface vaporization. Consider a laser pulse that has the simple time behavior shown in Fig. 18 and uniformly irradiates the surface of the material. The pulse length is t_p and the intensity is such that, combined with the reflectance, the absorbed power density is F_0. Again we assume that the optical energy is absorbed in a very thin layer at the surface. Let D_p be the diffusion length associated with the time t_p. The question is whether a significant amount of surface vaporization will occur before the pulse ends. One approach would be to use Eq. (46) to calculate the surface temperature at the time t_p and compare it to this vaporization temperature. However, this would ignore the influence of the latent heats of melting and of vaporization, which have an important influence. We shall discuss thermal flow with phase changes later. For the present purpose
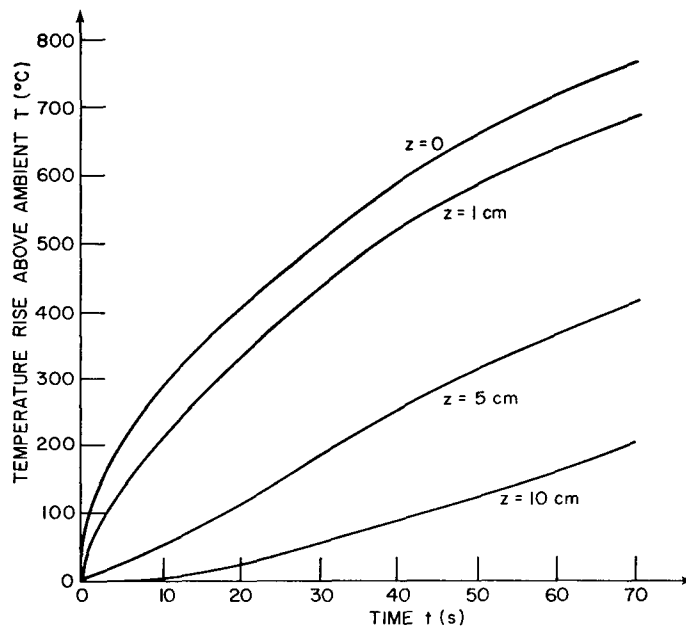
Fig. 17—Laser-induced temperature rise on front surface of
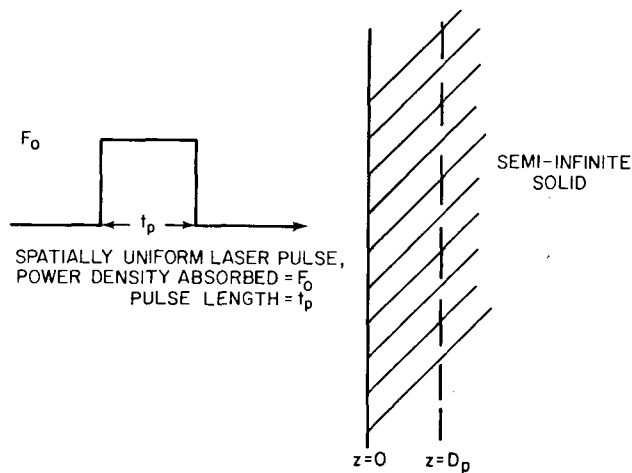aluminum as a function of time

Fig. 18—Irradiation of a semi-infinite solid by a pulse

we can include them by considering the energy required to melt and vaporize a portion of the material. The key is to estimate what thickness of the material is involved, and in this order-of-magnitude argument we simply use the thermal diffusion length for this thickness. Thus we set the criterion for vaporization as

$$\frac{F_0 t_p}{D_p} \geqslant \rho[C_s(T_m - T_0) + L_m + C_\ell(T_b - T_m) + L_v]$$

where ρ is density of the material, C_s and C_ℓ are the specific heats of the solid and liquid, respectively, T_m is the melting point, T_b is the boiling point, and L_m and L_v are the heats of melting and vaporization. Notice we are ignoring differences between the solid and liquid for density and conductivity, as is appropriate in this crude argument. If numerical values are checked, L_v dominates the expression on the right side of the inequality. For example, for aluminum L_v = 10,875 J/g, whereas all the other terms contribute a total of 3,046 J/g. Since the argument is crude, then, one usually takes

$$\frac{F_0 t_p}{D_p} \geqslant \rho L_v$$

as the criterion for vaporization by a pulse. Since $D_p = 2\sqrt{\kappa t_p}$, we have

$$F_0 \geqslant \text{approx } \frac{2\sqrt{\kappa}\, L_v \rho}{\sqrt{t_p}}. \tag{51}$$

Some calculations based on Eq. (51) are shown in Fig. 19. Most metals fall in the band indicated. For a given pulse time, at power densities greater than the band indicates, vaporization effects would be expected to be important. Some useful thermal constants are included in Table 2.
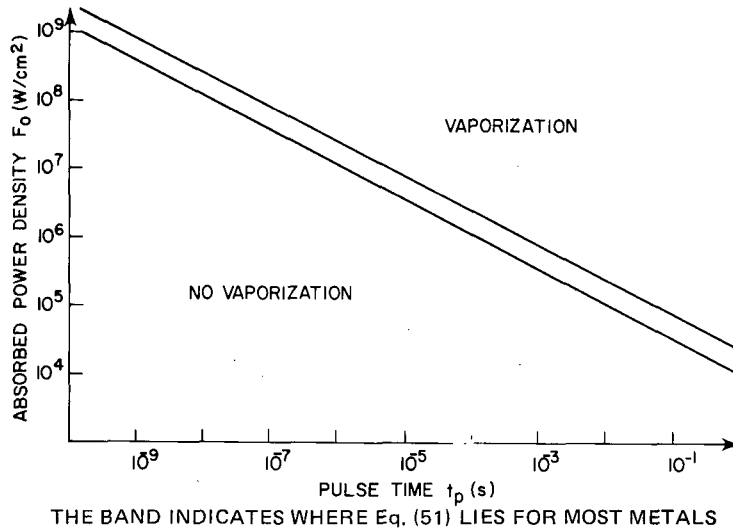

THE BAND INDICATES WHERE Eq. (51) LIES FOR MOST METALS

Fig. 19—Power density—pulse time criterion for vaporization

Table 2
Thermochemical Data for Metals*

Metal or Alloy	Diffusivity† (cm²/s)	Conductivity†		Specific Heat†‡		Density (g/cm³)	Solidus Temperature (°C)	Liquidus Temperature (°C)	Heat of Melting		Vaporization Temperature (°C)	Heat of Vaporization	
		(W/cm K)	(cal/s cm K)	(J/g K)	(cal/g K)				(J/g)	(cal/g)		(J/g)	(cal/g)
Al	0.85	2.40	0.57	1.05	0.25	2.7	--	660	400	95.6	2,520	10,875	2,600
2024 Al	0.60	1.732	0.414	1.0	0.24	2.77	502	638	--	--	--	--	--
Ti	0.0636	0.216	0.0516	0.753	0.18	4.51	--	1,670	324	77.3	3,289	8,790	2,100
Ti (6Al, 4V)	0.051	0.19	0.0455	0.837	0.20	4.47	1,537	1,649	--	--	--	--	--
Fe	--	--	--	--	--	7.86	--	1,536	247	59.1	2,862	6,260	1,496
304 Stainless Steel	0.0523	0.259	0.062	0.628	0.15	8.0	1,399	1,454	--	--	--	--	--

*Data compiled by R. L. Stegman of the Naval Research Laboratory, Washington, D.C.
†These values represent an average over the temperature between room temperature and the melting point.
‡Of the solid.

In deriving Eq. (51), we have been seeking the power density required, at a given pulse length, for a thermal layer to be vaporized. The same expression, of course, tells us the pulse time at which vaporization becomes important for a fixed power density. Rewriting Eq. (51) gives for this time

$$t_p > \text{approx} \; \frac{K^2 T_{\text{vap}}^2 \pi}{4 F_0^2 \kappa}. \tag{52}$$

Let us compare this to the time required for surface vaporization to begin. We do this by using our solution for heat flow in the semi-infinite solid for the surface (Eq. (46)) and solving for the time at which the front surface reaches the vaporization temperature:

$$T_{\text{vap}} = \frac{2 F_0}{K} \sqrt{\frac{\kappa t_{\text{vap}}}{\pi}}$$

or

$$t_{\text{vap}} = \frac{K^2 T_{\text{vap}}^2 \pi}{4 F_0^2 \kappa}.$$

Thus, at $t_p = t_{\text{vap}}$ this calculation would predict that vaporization at the surface begins. For example, at $F_0 = 10^6$ W/cm^2, vaporization begins at $t_p \approx 10^{-5}$ to 10^{-6} s, depending on the metal. On the other hand, for a thermal layer to be evaporated requires, according to Eq. (52), $t_p \approx 10^{-3}$ s. It turns out that both estimates are useful. In a later section we shall discuss features of a more correct treatment, which accounts for both the heat of melting and the heat of vaporization in the dynamic situation of propagating solid—liquid and liquid—vapor interfaces.

3.3. No Phase Change—Slab of Finite Thickness

Let us turn now to a treatment of another geometry which can be useful in practical cases, namely irradiation of one surface of a sheet or slab of finite thickness. Let the slab be taken as infinite in extent in the x and y direction, and let the laser irradiation be uniform over the entire surface $z = 0$. Thus we again have a one-dimensional situation, as shown in Fig. 20. The thickness of the sheet is taken as ℓ, the absorbed power density as a function of time is $F(t)$, and we again assume that the radiation is absorbed in a very narrow layer at the front surface. The equation we wish to solve is, then,

$$\frac{\partial^2 T}{\partial z^2} - \frac{1}{\kappa} \frac{\partial T}{\partial t} = 0$$

with the boundary conditions

$$-K \left. \frac{\partial T}{\partial z} \right)_{z=0} = F(t)$$

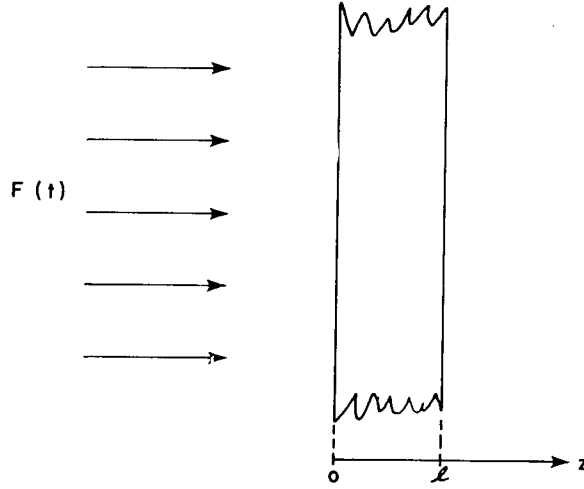$$-K \left. \frac{\partial T}{\partial z} \right)_{z=\ell} = 0.$$

Fig. 20—Irradiation of a slab of finite thickness

The second boundary condition states that the rear surface is insulated. We shall look at the consequences of this assumption a little later.

As we showed for the semi-infinite slab, the solutions turn out to be elaborate. Turning to the special case of $F(t) = F_0$, a constant, the solution is

$$T(z, t) = \frac{F_0 \kappa}{K\ell} t + \frac{F_0 \ell}{K} \left\{ \frac{3(\ell - z)^2 - \ell^2}{6\ell^2} - \frac{2}{\pi^2} \sum_{n=1}^{\infty} \frac{(-1)^n}{n^2} e^{-\kappa n^2 \pi^2 t/\ell^2} \cos\left[\frac{n\pi(\ell - z)}{\ell}\right] \right\}.$$

(53)

We can check that this satisfies the boundary conditions:

$$\frac{\partial T}{\partial z} = \frac{F_0 \ell}{K} \left\{ \frac{-(\ell - z)}{\ell^2} - \frac{2}{\pi^2} \sum_{n=1}^{\infty} \frac{(-1)^n}{n^2} e^{-\kappa n^2 \pi^2 t/\ell^2} \frac{n\pi}{\ell} \sin\left[\frac{n\pi(\ell - z)}{\ell}\right] \right\}.$$

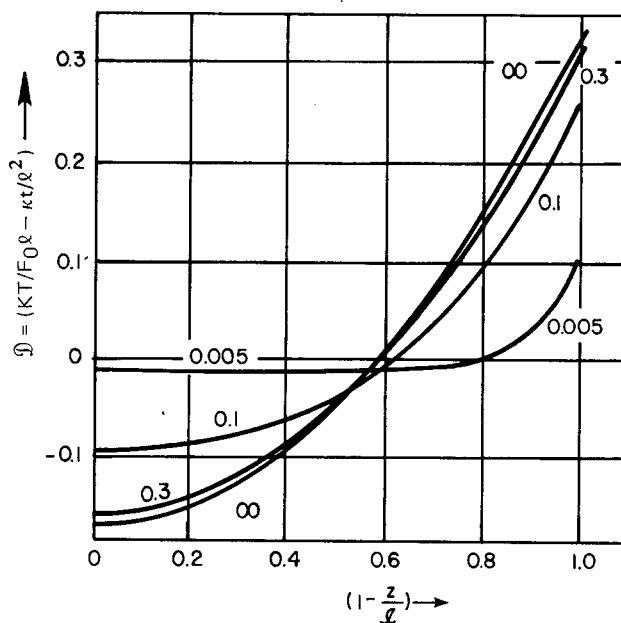Now $\sin(n\pi) = 0$ and $\sin(0) = 0$, so the Σ term vanishes at both $z = 0$ and $z = \ell$, and

$$\left. \frac{\partial T}{\partial z} \right)_{z=0} = -\frac{F_0}{K}$$

$$\left. \frac{\partial T}{\partial z} \right)_{z=\ell} = 0.$$

Similarly, the thermal diffusion equation is satisfied, as the reader can verify.

Let us look briefly at this solution. It consists of a linear term in t, together with a "correcting term," which can be plotted as shown in Fig. 21. In other words, what is plotted is the term

34

NOTE THAT $0 < z < \ell$. THE NUMBERS ON THE CURVES ARE VALUES OF $\kappa t / \ell^2$

Fig. 21—$\mathfrak{D}$ as a function of $1 - z/\ell$ (Ref. 5, p. 113)

$$\mathfrak{D} = \frac{3(\ell-z)^2 - \ell^2}{6\ell^2} - \frac{2}{\pi^2} \sum_{n=1}^{\infty} \frac{(-1)^n}{n^2} e^{-\kappa n^2 \pi^2 t/\ell^2} \cos\left[\frac{n\pi(\ell-z)}{\ell}\right].$$

Let us examine some special cases. At $z = 0$, for example,

$$T(o, t) = \frac{F_0 \kappa}{K\ell} t + \frac{F_0 \ell}{K}\left[\frac{1}{3} - \frac{2}{\pi^2} \sum_{n=1}^{\infty} \frac{1}{n^2} e^{-\kappa n^2 \pi^2 t/\ell^2}\right]. \tag{54}$$

We can rewrite this as

$$T(o, t) = \frac{F_0 \kappa}{K\ell} t + \frac{F_0 \ell}{K} \mathfrak{D}_{z=0}.$$

Now $\mathfrak{D}$ at a fixed value of z is a function of $\kappa t/\ell^2$. If $\eta = \kappa t/\ell^2$, we can write

$$T(o, t) = \frac{F_0 \ell}{K}(\eta + \mathfrak{D}_{z=0}(\eta)). \tag{55}$$

35

Figure 22 shows how $\mathfrak{D}$ depends on η, for $z = 0$, and was taken from the previous graph of $\mathfrak{D}$ vs $(1 - z/\ell)$ (Fig. 21). Note that at small η, i.e., at $\kappa t \ll \ell^2$, $\mathfrak{D} \approx 0$, so that the front surface initially heats up linearly with time, as
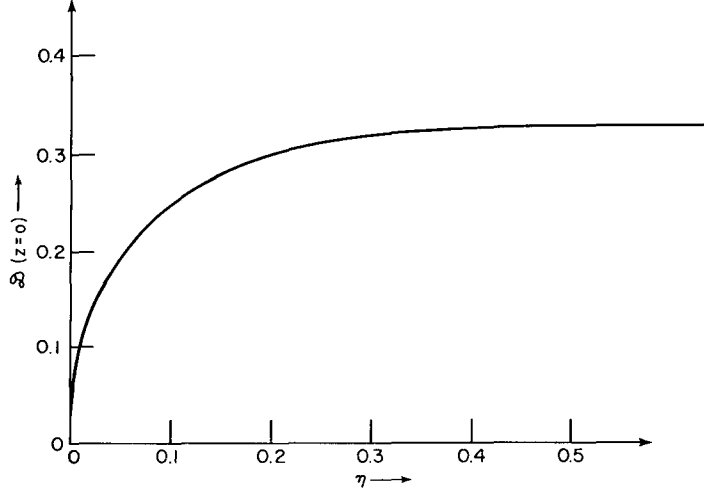
$$T(o, t) = \frac{F_0 \kappa}{K \ell} t. \tag{56}$$

Fig. 22— $\mathfrak{D}$ at $z = 0$ as a function of η

For large t values, or $\kappa t \gg \ell^2$, $\mathfrak{D}_{z=0}$ approaches a limiting value of about 0.33. Thus at long times

$$T(o, t) = \frac{F_0 \ell}{K} \left(\frac{\kappa t}{\ell^2} + 0.33 \right), \quad \kappa t \gg \ell^2. \tag{57}$$

Here again we see linear behavior, but this time there is an additive constant. If we have a very thick slab, we should get the same result as our previous solution for the time to reach $600°C$ on the front surface of aluminum with an absorbed power density of 200 W/cm^2. It turns out that the limiting form of Eq. (56) is not correct because it ignores the behavior of $\mathfrak{D}_{z=0}(\eta)$ at small η. It is necessary to use the full expression. Thus

$$\eta + \mathfrak{D}_{z=0}(\eta) = \frac{KT}{F_0 \ell}.$$

Assume that $\ell = 100$ cm, since we know from our infinite-slab solution that the diffusion distance is 12 cm at $T = 600°C$ on the front. Thus

$$\eta + \mathfrak{D}_{z=0}(\eta) = \frac{2.3 \times 600}{200 \times 100} = 0.069.$$

Reading very roughly from the graph of $D_{z=0}$ vs η gives

36

$$\eta \approx 0.004 \quad \text{at} \quad \mathcal{D} \approx 0.065.$$

Thus our solution is

$$\eta \approx 0.004 = \frac{\kappa t}{\ell^2},$$

which gives, since $\kappa \approx 0.9$ cm^2/s, a time of about 44 s, in reasonable agreement with the semi-infinite-slab solution.

Now let us turn to a consideration of the rear surface temperature. For this case, $z = \ell$, so Eq. (53) becomes

$$T(\ell, t) = \frac{F_0 t \kappa}{K \ell} + \frac{F_0 \ell}{K} \left[-\frac{1}{6} - \frac{2}{\pi^2} \sum_{n=1}^{\infty} \frac{(-1)^n}{n^2} e^{-\kappa n^2 \pi^2 t / \ell^2} \right]$$

or, introducing η as before, we have

$$T(\ell, t) = \frac{F_0 \ell}{K} (\eta + \mathcal{D}_{z=\ell}(\eta)).$$

Comments could be made here for the rear surface temperature, and they would be similar to those we made for the front surface temperature. It is interesting to compare the front surface temperature to the back surface temperature. This has a simple form for thin sheets, where $\kappa t / \ell^2 \gg 1$. By referring to the graph (Fig. 21) of $\mathcal{D}$ vs $(1 - z/\ell)$, one can read off values for $\mathcal{D}_{z=\ell}(\infty)$ and $\mathcal{D}_{z=0}(\infty)$, and thus

$$T(o, t) - T(\ell, t) \approx 0.5 \frac{F_0 \ell}{K}$$

for

$$\kappa t / \ell^2 \gg 1.$$

Notice in Fig. 21 that the limiting values are approached rapidly; they are nearly realized by the time $\kappa t / \ell^2 = 1$. As a numerical illustration, if we have 0.3-cm-thick aluminum,

$$T(o, t) - T(\ell, t) \approx 13°\text{C}$$

For the same numbers we used above. This situation, with the two surfaces heating at the same rate but separated by 13°C, would start at a time of the order of $t \approx \ell^2 / \kappa \approx 0.1$ s. At this time the front surface temperature is about 35°C.

Let us turn now to a different sort of heat input. So far we have been discussing continuous irradiation. Another simple case, which is a reasonable approximation under certain conditions, is that of a laser pulse which is short enough to be treated as a delta function. Take again a slab of thickness ℓ, and assume that the energy is deposited in a very thin layer near the surface. F refers, as before, to the fraction absorbed by the material. The laser power density, that is, must be multiplied by the optical absorptance. In this case we solve the thermal diffusion equation subject to the boundary condition that

$$-K \left.\frac{\partial T}{\partial z}\right)_{z=0} = -K \left.\frac{\partial T}{\partial z}\right)_{z=\ell} = 0,$$

with the stipulation that there is an instantaneous release of E_0 units of energy per unit area in the plane $z = 0$ at time zero. This type of problem is discussed in Carslaw and Jaeger [5] and is most easily solved by Laplace transform methods. For our present purpose we quote the solution

$$T(z, t) = \frac{E_0 \kappa}{K \ell} \left[1 + 2 \sum_{n=1}^{\infty} \cos\left(\frac{n\pi z}{\ell}\right) e^{-\kappa n^2 \pi^2 t / \ell^2} \right]. \tag{58}$$

In Eq. (58) we have introduced E_0, the energy per unit area in the pulse. Thus,

$$E_0 = \int_0^{\infty} F(t) \, dt.$$

For the case under consideration, $F(t)$ is considered to be a delta function.

Equation (58) is the basis for a scheme used quite frequently for the measurement of thermal parameters [6]. This scheme consists of using a thin sheet of the material to be studied and irradiating uniformly one surface with a very short laser pulse while monitoring the temperature rise induced on the back surface. If one knows E_0, and if the assumptions of no heat loss are valid, the experiment can yield values of both specific heat and thermal conductivity. One adjusts the pulse energy, and hence E_0, so that the induced temperature rise is small. In this way the values of specific heat and thermal conductivity are representative of essentially the ambient temperature of the material.

To see how this is applied, rewrite Eq. (58) for the back surface, $z = \ell$:

$$T(\ell, t) = \frac{E_0 \kappa}{K \ell} \left[1 + 2 \sum_{n=1}^{\infty} (-1)^n e^{-\kappa n^2 \pi^2 t / \ell^2} \right]. \tag{59}$$

If we introduce a characteristic time $t_c = \ell^2 / \kappa \pi^2$, Eq. (59) looks approximately like the curve shown in Fig. 23. Here we have also introduced a characteristic temperature $T_c = E_0 \kappa / K \ell$ and plotted T/T_c vs t/t_c, or

$$\frac{T}{T_c} = 1 + 2 \sum_{n=1}^{\infty} (-1)^n e^{-n^2 t / t_c}. \tag{60}$$

Essentially the experiment consists of monitoring the temperature as a function of time and fitting it to Eq. (60). This can be done quite readily. First, the long-term temperature rise T_∞ yields the specific heat because
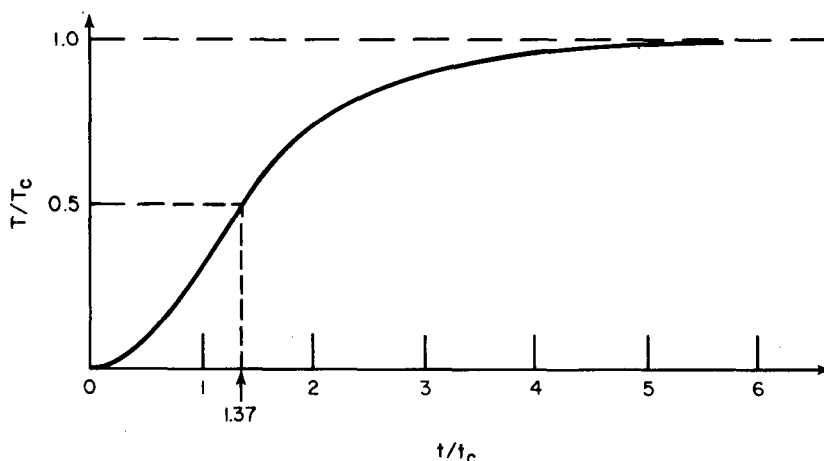
$$\frac{T_\infty}{T_c} = 1$$

Fig. 23—Normalized back surface temperature response to
a delta function heat pulse

and, on substituting for T_c,

$$T_\infty = \frac{E_0 \kappa}{K \ell} \; ;$$

or, since $\kappa = K/\rho C$,

$$C = \frac{E_0}{T_\infty \rho \ell} . \tag{61}$$

This technique of measuring specific heat is, of course, not unique to pulsed lasers. It is sometimes referred to as the slab calorimeter. The accuracy of the method depends on knowing E_0, which is frequently difficult to ascertain with laser radiation. In some applications Eq. (61) is used to calculate E_0, the energy actually absorbed from the laser pulse, by using materials of known specific heat.

The pulsed laser measurement technique is especially suited to determining thermal diffusivity. The magnitude of the back surface temperature rise depends, as we saw, on the energy which is coupled into the material, and this may be difficult to know with any precision. However the time dependence of the back surface temperature is independent of the energy input and is controlled only by the diffusivity κ. A simple way to derive κ from a temperature-time profile can be seen from Fig. 23. One measures the time required for the measured temperature response to reach some fraction, say one-half, of its limiting value. Let us call this time $t_{1/2}$. It can be shown numerically [6] from Eq. (60) that

$$\frac{T}{T_c} = \frac{1}{2} = 1 + 2 \sum_{n=1}^{\infty} (-1)^n e^{-n^2 t_{1/2}/t_c}$$

is satisfied when

$$t_{1/2}/t_c = 1.37 .$$

Using $t_c = \ell^2/(\kappa\pi^2)$ yields

$$\kappa = \frac{1.37}{\pi^2} \frac{\ell^2}{t_{1/2}} . \tag{62}$$

Thus a measurement of $t_{1/2}$, together with the thickness of the specimen, immediately gives the thermal diffusivity. If one knows E_0 this experiment gives values of both the specific heat and the diffusivity, and hence if one knows the density ρ the experiment gives the thermal conductivity.

This technique has been applied often at rather high temperatures, usually in the $1000°C$ range and above. At these temperatures steady-state methods of measuring the thermal conductivity are difficult to apply because radiation losses are so large. In the laser flash technique the radiation loss goes like $T_\infty^4 - T_0^4$, where T_0 is the starting or ambient temperature, established by, say, a furnace, and T_∞ is defined above. This radiation loss can be made quite small by adjusting E_0 so that T_∞ is only a few degrees larger than T_0. Since the precise value of E_0 is difficult to establish, these experiments typically measure only the thermal diffusivity, not the conductivity.

A final remark on the criterion for the applicability of Eq. (60) to slab heating concerns the limits on the laser pulse duration. No laser pulse is, of course, a true δ function. Our solution would be expected to be correct for laser pulse times which are short compared to the time it takes the back surface to respond. The response times are of the order of t_c, so we have the criterion

$$t_p \ll t_c$$

or

$$t_p \ll \ell^2/(\kappa\pi^2) .$$

Calculations that include explicitly the time dependence of the laser pulse [7] indicate that our δ-function solution is in error by less than about 2% provided that t_p is less than or equal to about 4% of t_c. Some typical values of t_c with specimens 1 mm thick are given below.

	κ (cm^2/s)	$t_c = \ell^2/\kappa\pi^2$ (ms)
Aluminum	0.85	1.2
Stainless steel	0.0523	19

Typical laser pulse lengths are about 1/2 to 1 ms for the so-called "normal mode" lasers, and thus with 1-mm-thick specimens the technique would be fairly accurate for stainless steel but not very good for aluminum. Thicker specimens would help, but this would make the rear surface temperature rise smaller. If our laser pulse has, say, 20 J/cm^2 in it and we use the 10.6-μm absorptance quoted earlier for as-received surfaces, the anticipated temperature rises at the back of the 1-mm specimens would be as shown below.

	α	E_0 (J/cm^2)	ρ (g/cm^2)	C (J/g$^\circ$C)	$T_\infty = E_0/\rho C\ell$ ($^\circ$C)
Aluminum	0.04	0.8	2.7	1.05	2.8
Stainless steel	0.4	8.0	8.0	0.628	16

We see the need to use shorter laser pulses but with the same amount of energy. Another solution would be to carry out a more detailed heat-flow calculation. Both tailoring of the pulse shape and more detailed calculations are usually employed in current applications of laser flash techniques [8].

3.4. Melting

Consider first the case of a semi-infinite slab melted, with instantaneous melt removal, as indicated in Fig. 24.
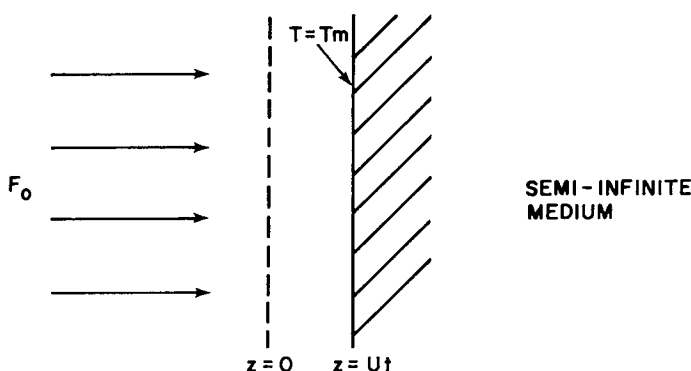
Fig. 24—Irradiation of a semi-infinite slab with
instantaneous melt removal

We solve this by considering ourselves moving along with the interface. But to do this we have to reconsider our heat-flow equation, which is

$$\frac{\partial^2 T}{\partial z^2} - \frac{1}{\kappa} \frac{\partial T}{\partial t} = 0.$$

Recall that this was derived by noting the rate at which heat accumulated in an elemental volume:

$$\rho C \frac{\partial T}{\partial t} + \frac{\partial}{\partial z} \left(-K \frac{\partial T}{\partial z} \right) = 0.$$

If the medium is moving, an additional amount of heat $\rho C T$ is flowing in at rate V. So

41

$$-K \frac{\partial T}{\partial z} \quad \text{becomes} \quad -K \frac{\partial T}{\partial z} + V\rho C T.$$

Thus, for moving media, the heat-flow equation is

$$\rho C \frac{\partial T}{\partial t} + \frac{\partial}{\partial z} \left(-K \frac{\partial T}{\partial z} + V\rho C T \right) = 0,$$

provided we are not generating any heat in the solid.

Thus

$$\frac{\partial T}{\partial t} - \kappa \frac{\partial^2 T}{\partial z^2} + V \frac{\partial T}{\partial z} = 0. \tag{63}$$

So we can find at least a steady-state solution to the problem by basing our coordinate system at the interface and letting the material flow in at some rate to be determined. Call the rate $-U$, where U is a positive number. The solution will be

$$T = T_m e^{-Uz'/\kappa} \tag{64}$$

where κ is diffusivity of the solid, T_m is the melting temperature, and z' is the distance from the melting front. That is, this is the solution to

$$\frac{\partial T}{\partial t} - \kappa \frac{\partial^2 T}{\partial z'^2} - U \frac{\partial T}{\partial z'} = 0,$$

as we can verify. First, $\partial T/\partial t = 0$ because this is the steady-state profile, or

$$\kappa \frac{\partial^2 T}{\partial z'^2} + U \frac{\partial T}{\partial z'} = 0. \tag{65}$$

Of course $T = T_m$ at $z' = 0$, and $T \to 0$ as $z' \to \infty$. It is trivial to show, by differentiation, that Eq. (64) is the solution to Eq. (65).

To calculate U, we use energy balance. F_0 must raise the material to T_m, its melting point ($T_m°C$ above ambient), and then melt it. Thus in time Δt the energy put into thickness $\Delta z'$ (where $U = \Delta z'/\Delta t$) must be given by

$$\frac{F_0 \Delta t}{\Delta z'} = L\rho + C T_m \rho$$

or

$$F_0 = \rho [L + C T_m] U. \tag{66}$$

Thus we can write, for the steady-state temperature profile,

$$T = T_m \exp\left\{-\frac{z'}{\kappa}\left[\frac{F_0}{\rho(L + CT_m)}\right]\right\} \tag{67}$$

where $F_0/[\rho(L + CT_m)]$ is the velocity of the melting front. This solution also would be appropriate to sublimation, where L is then the heat of sublimation and T_m the sublimation temperature. Note that this is the semi-infinite-slab approximation and cannot be used to estimate the time to penetrate a slab of given thickness.

Let us consider aluminum, with $F_0 = 200$ W/cm^2. Taking a more accurate value of the melting point than in earlier examples, $T_m = 640°$C (the actual melting point of $660°$C minus room temperature of $20°$C). If we put in the other values of the parameters, T falls off as shown in Fig. 25.
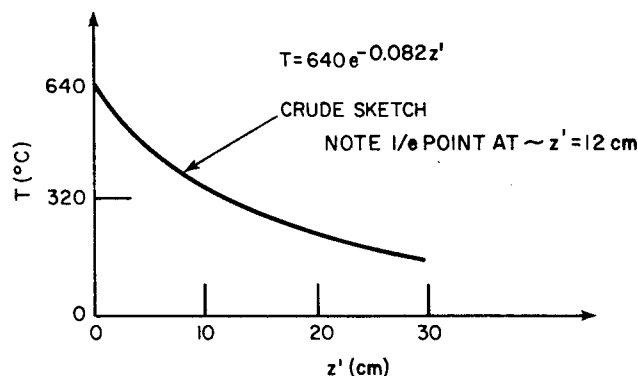

Fig. 25—Temperature profile in aluminum with instantaneous melt removal

As another illustration, consider plexiglass. Plexiglass is rapidly eroded by 10.6-μm laser radiation, by a process that is essentially sublimation. Since it couples extremely well ($\mathfrak{a} \approx 1.0$) and has a very low thermal diffusivity ($\kappa \approx 10^{-4}$ cm^2/s), it can be used to make "burn patterns" of the beam. That is, the depth of the erosion at a given point is linearly proportional to the energy density incident at that point. We can understand this by applying heat-flow concepts. Let us apply Eq. (67) and interpret L as the heat of erosion. Since $C \approx 1.1$ J/g-$°$C and $T_m \approx 200°$C and $L \approx 1000$ J/g, for a crude calculation we can ignore CT_m. The density is about 1.1 g/cm^3. We then have

$$T \approx 200\, e^{-9F_0 z'}.$$

Since $\mathfrak{a} \approx 1$, for a typical power density like 5 kW/cm^2 we have $F_0 = 5 \times 10^3$, so that

$$T \approx 200\, e^{-4.5 \times 10^4 z'}.$$

Hence the temperature profile is confined to an extremely narrow region near the eroding surface. The rate of erosion is, by Eq. (66) with CT_m ignored,

$$U \approx 4.5 \text{ cm/s}.$$

Now we can see why plexiglass is useful for monitoring the beam profile, and why it can pick up fairly fine structure in the beam. After irradiation for a time t the penetration depth is $Ut = (F_0 t)/(\rho L)$, and this should be large compared to a thermal diffusion length $D = 2\sqrt{\kappa t}$ if the pattern is to reveal fine structure. Otherwise thermal diffusion would "wash out" the pattern by distributing the energy in a radial direction. Thus

$$2\sqrt{\kappa t} << \frac{F_0 t}{\rho L}.$$

For the numbers we used above at $t \approx 1/4$ s, we have a depth of 1 cm. Thus

$$2\sqrt{10^{-4} \times \frac{1}{4}} \approx 0.1 \text{ mm} << 1 \text{ cm}$$

and we see the criterion is well satisfied.

Let us look at a more complete problem, namely melting by laser radiation of a slab of material. One basic problem is what happens to the melted material. (We will ignore the vaporization question for now.) There are two cases which are fairly amenable to numerical solution. They are the "fully retained liquid" case, in which all the liquid is presumed to stay in place, and the "full ablation" case, in which the melt is presumed to disappear magically as soon as it forms. The latter case might correspond to the presence of a heavy windstream which blows away the melt.

Looking first at the full ablation case, we have the situation shown in Fig. 26. T_2 is the temperature in the solid, and the front surface at $z = 0$ first warms up to the melting point T_m (above ambient) and then begins to move to the right. S denotes its position as a function of time. When $S = \ell$, the process is over, and we call this time t_f. We denote by t_m the time at which the front surface begins to melt. The field equation is
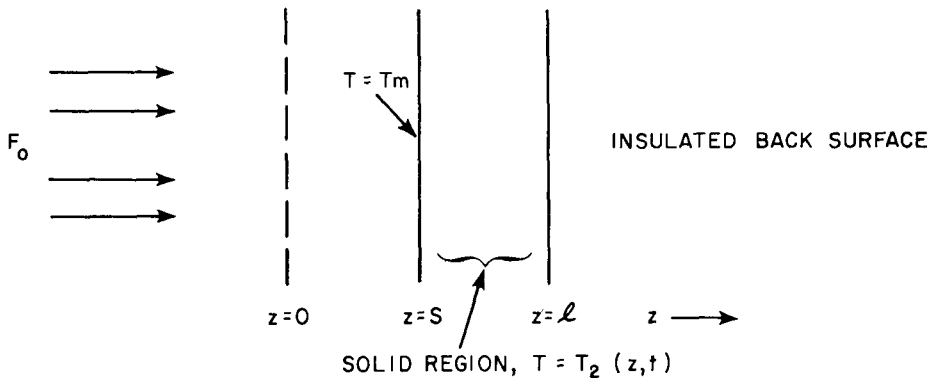

Fig. 26—Fully ablated case

$$\frac{\partial^2 T_2}{\partial z^2} - \frac{1}{\kappa_2} \frac{\partial T_2}{\partial t} = 0 \quad \text{for} \quad 0 \leqslant t \leqslant t_f.$$

The boundary conditions are

$$K_2 \left. \frac{\partial T_2}{\partial z} \right)_{z=0} = -F_0 \quad \text{for} \quad 0 \leqslant t \leqslant t_m$$

$$K_2 \left. \frac{\partial T_2}{\partial z} \right)_{z=S} = -F_0 + \rho L \frac{dS}{dt} \quad \text{for} \quad t_m \leqslant t \leqslant t_f$$

$$K_2 \left. \frac{\partial T_2}{\partial z} \right)_{z=\ell} = 0 \quad \text{for} \quad 0 \leqslant t \leqslant t_f.$$

The starting conditions are

$$T_2(z, o) = T_{20}$$

$$S)_{t \leqslant t_m} = 0.$$

The above boundary conditions are nonlinear, and a solution in analytical form is very difficult. This is due to the presence of the moving boundary and appears in the second boundary condition, which states that the boundary moves at a rate dS/dt determined by a balance between the heat of melting L, the heat input F_0, and the heat flow by thermal conduction.

One relationship must hold for this problem; it follows from energy balance. The total energy put in per unit area is $F_0 t_f$, and, since the material is simply heated to T_m and melted, this energy goes solely to those processes. Thus

$$F_0 t_f = \rho (L + C T_m).$$

This is convenient, for one can check numerical solutions. More important, it gives a first-order estimate of the time needed to melt through materials by laser radiation.

Turning now to the fully retained liquid case, we have the following set of equations. The definitions are the same as above, except that subscript 1 now refers to the molten state, whereas subscript 2 is still the solid state (see Fig. 27). The field equations are

$$\frac{\partial^2 T_2}{\partial z^2} - \frac{1}{\kappa_2} \frac{\partial T_2}{\partial t} = 0 \quad 0 \leqslant t \leqslant t_f \quad \text{(solid)}$$

$$\frac{\partial^2 T_1}{\partial z^2} - \frac{1}{\kappa_1} \frac{\partial T_1}{\partial t} = 0 \quad t_m \leqslant t \leqslant t_f \quad \text{(liquid)}.$$
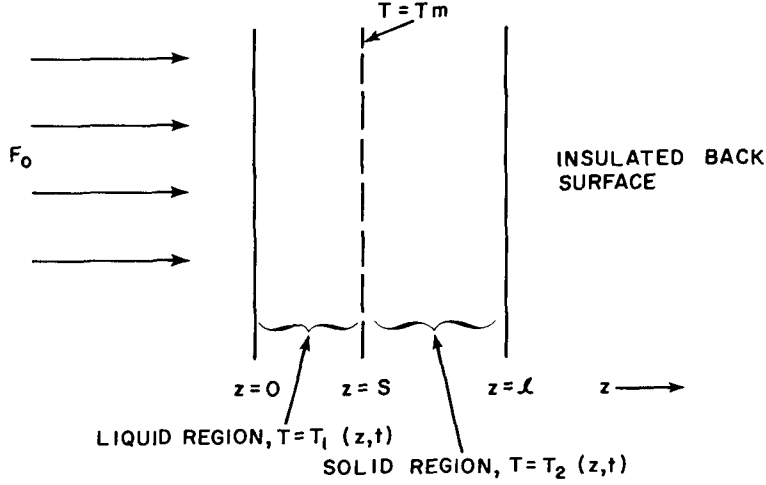
The boundary conditions are

45

Fig. 27—Fully retained liquid case

$$- K_2 \left. \frac{\partial T_2}{\partial z} \right)_{z=0} = F_0 \qquad 0 \leqslant t \leqslant t_m$$

$$- K_1 \left. \frac{\partial T_1}{\partial z} \right)_{z=0} = F_0 \qquad t_m \leqslant t \leqslant t_f$$

$$K_1 \left. \frac{\partial T_1}{\partial z} \right|_{z=S} - K_2 \left. \frac{\partial T_2}{\partial z} \right)_{z=S} = -\rho L \frac{dS}{dt} \qquad t_m \leqslant t \leqslant t_f$$

$$K_2 \left. \frac{\partial T_2}{\partial z} \right)_{z=\ell} = 0 \qquad 0 \leqslant t \leqslant t_f$$

$$T_2)_{z=S} = T_1)_{z=S} = T_m \qquad t_m \leqslant t \leqslant t_f.$$

The initial conditions are

$$T_2(z, o) = T_{20}$$

$$S)_{t \leqslant t_m} = 0.$$

Rather than discuss this problem in detail, we pass on to the more practical, although more complex, case of vaporization. For the fully retained liquid case, suffice it to say that the retained liquid has a shielding effect, and this causes the time to reach melting at the back surface to be longer than in the ablated model. Some typical values of melt-through time for 0.2-cm-thick material with $F_0 \approx 2$ kW/cm^2 are given below.

	Ablated (s)	Retained (s)
Aluminum	0.32	0.37
Stainless steel	4.0	4.5

3.5. Melting and Vaporization

We present here without derivation some results for the case of a slab of material, insulated on the surfaces, subjected to uniform and continuous irradiation [9]. These are one-dimensional calculations. It is assumed that the melt is fully retained until it reaches the vaporization temperature, where it disappears. Then we have the case illustrated in Fig. 28.
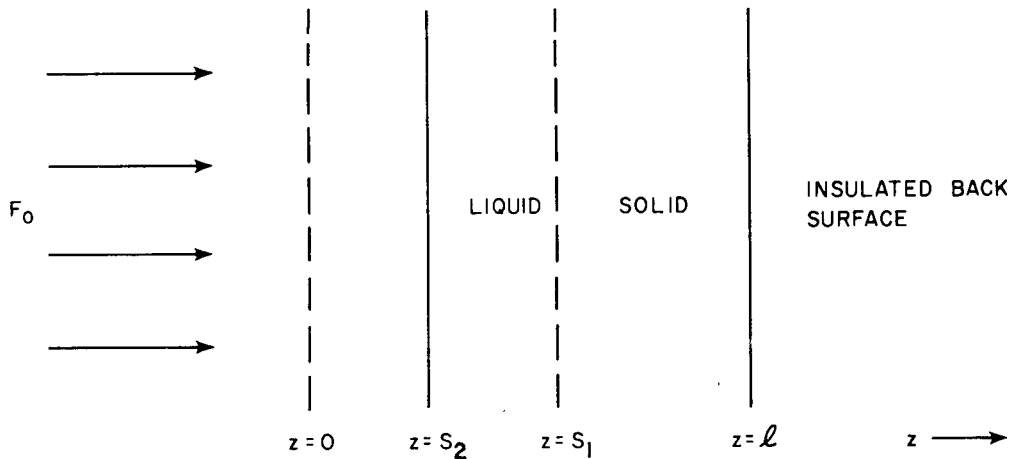
Fig. 28—Melting and vaporization, with fully retained liquid

Here S_2 is the position of the liquid-vapor interface and S_1 the position of the solid-liquid interface. This problem has been solved numerically at NRL [9], and we shall show some results. The assumptions are that in each phase the thermal properties are independent of temperature. In the curves, the following definitions are used:

$$\alpha \hat{Q} = \frac{F_0 \ell}{\rho L \kappa_{\text{solid}}}$$

$$\tau = \frac{\kappa_{\text{solid}} t}{\ell^2}$$

$$\theta = (T - T_m) C_{\text{solid}} / L$$

47

L = latent heat of fusion

subscript 0 = ambient temperature

$\omega = L_v/L$, with L_v the latent heat of vaporization.

In these equations T is understood to be in degrees Celsius and represents the actual temperature. Although the thermal conductivities of liquid and solid are allowed to differ, the specific heats are assumed to be the same.

Note that when $F_0 \to 0$ and $F_0 \to \infty$, we get certain easy limits. For $F_0 \to 0$ no vaporization can take place, the melting is small, and we approach the fully ablated limit. On the other hand, as $F_0 \to \infty$, all the liquid should be vaporized by t_f, the time the back surface melts.

So in this limit

$$F_0 t_f = \rho\ell[L + (T_m - T_0)C_{\text{solid}} + (T_v - T_m)C_{\text{liquid}} + L_v] \qquad (F_0 \to \infty),$$

whereas

$$F_0 t_f = \rho\ell[L + (T_m - T_0)C_{\text{solid}}] \qquad (F_0 \to 0).$$

The limiting values are represented by the asymptotes of the curves (Figs. 29-31) indicated by dashed lines on the plots of $\alpha\hat{Q}$ vs τ. Note on these plots that the dashed lines are at $45°$, or have a slope of -1. These are log-log plots, so the asymptotes can be described by

$$\log(\alpha\hat{Q}) = \log \mathcal{C} - \log \tau_f$$

where $\mathcal{C} \to \mathcal{C}_\infty$ as $\alpha\hat{Q} \to \infty$, and $\mathcal{C} \to \mathcal{C}_0$ as $\alpha\hat{Q} \to$ zero. If we take the antilog,

$$\alpha\hat{Q} = \mathcal{C}\tau_f^{-1},$$

substituting in the definition of $\alpha\hat{Q}$ and τ_f gives

$$\frac{F_0\ell}{\rho L \kappa_{\text{solid}}} = \mathcal{C}\frac{\ell^2}{\kappa_{\text{solid}} t_f}$$

or

$$F_0 t_f = \rho\ell L\mathcal{C}.$$

By comparison with the $F_0 \to 0$ and the $F_0 \to \infty$ limits above we can see that

$$\mathcal{C}_0 = \frac{1}{L}[L + (T_m - T_0)C_{\text{solid}}]$$

and

$$\mathcal{C}_\infty = \frac{1}{L}[L + (T_m - T_0)C_{\text{solid}} + (T_v - T_m)C_{\text{liquid}} + L_v].$$
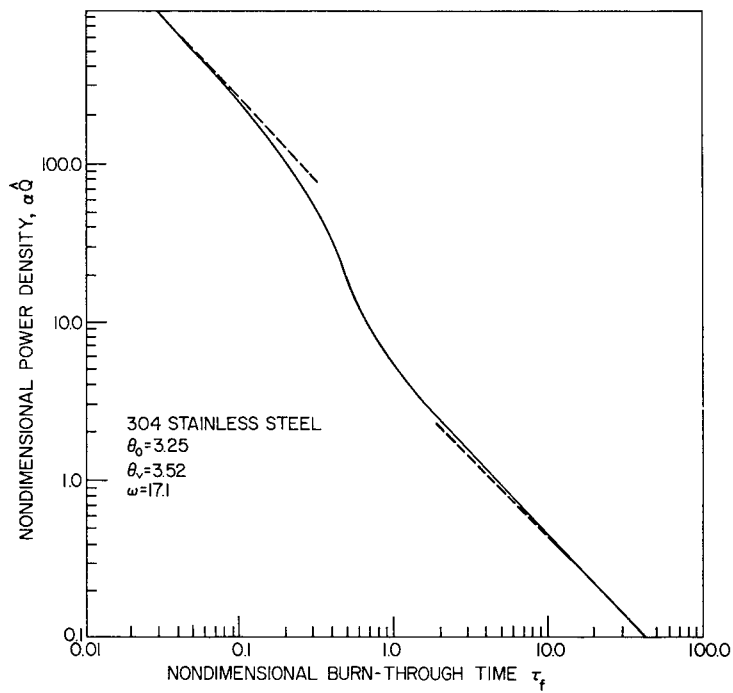
48

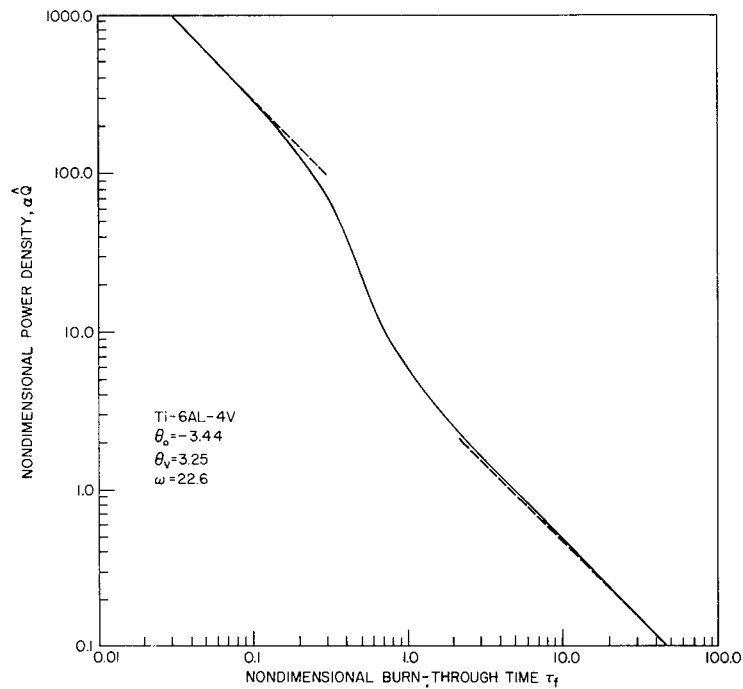Fig. 29—Power density vs burn-through time for
stainless steel (Ref. 9)

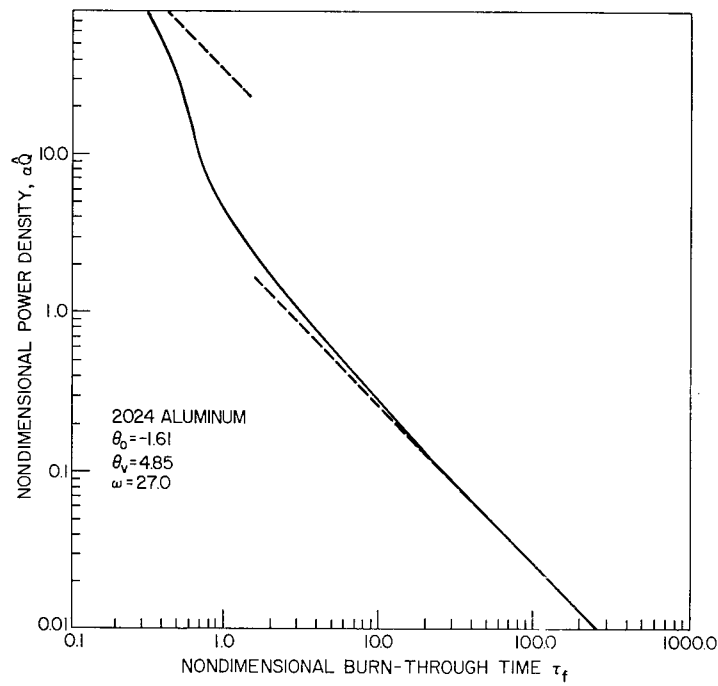Fig. 30—Power density vs burn-through time for
titanium alloy (Ref. 9)

Fig. 31—Power density vs burn-through time for
aluminum alloy (Ref. 9)

The numerical values of the thermal parameters which were used in generating these solutions are included as a separate table (Table 3) in addition to the graphs (Figs. 29-34).
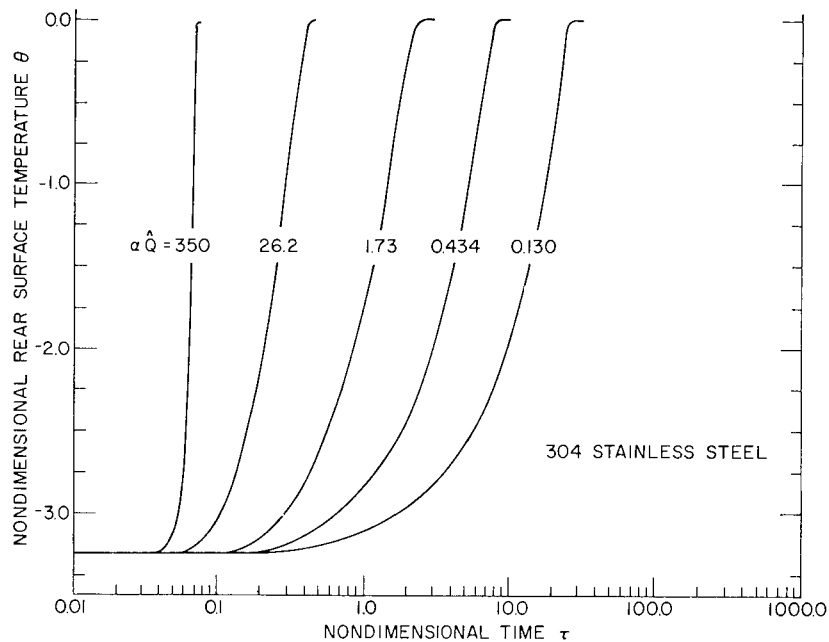
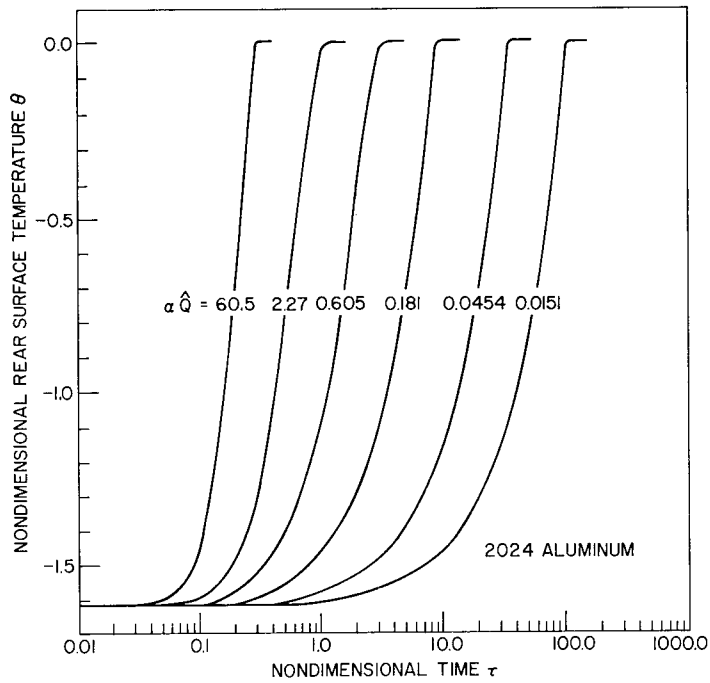Fig. 32—Rear surface temperature rise for stainless steel (Ref. 9)

Fig. 33—Rear surface temperature rise for aluminum
alloy (Ref. 9)
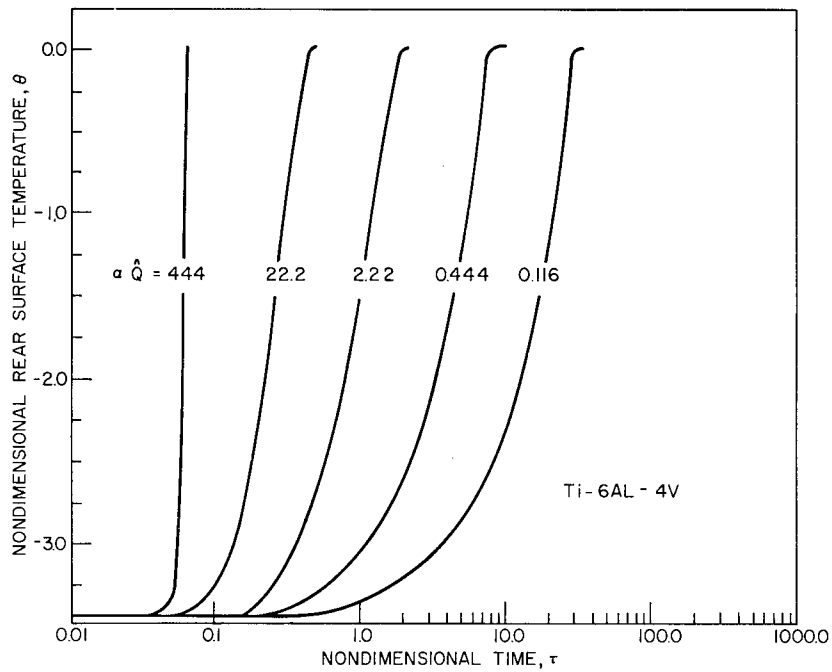
Fig. 34—Rear surface temperature rise for titanium alloy (Ref. 9)

Table 3

Metal or Alloy	T_m (°C)	T_v (°C)	L (cal/g)	L_v (cal/g)	ρ (g/cm³)	K_s (cal/s·cm·°C)	K_ℓ (cal/s·cm·°C)	c_s (cal/g·°C)	c_ℓ (cal/g·°C)	κ_s (cm²/s)	κ_ℓ (cm²/s)
304 Stainless steel	1,454	3,000	65	1,112	8.0	0.062	0.062	0.148	0.148	0.0523	0.0523
Ti (6Al, 4V)	1,649	3,285	94	2,124	4.47	0.0455	0.0455	0.199	0.199	0.051	0.051
2024 Alum.	638	2,480	95	2,565	2.77	0.414	0.207	0.249	0.249	0.6	0.3

Provided one knows F_0, these solutions are reasonable estimates for the time to penetrate a metal specimen with a laser beam. In application, however, one must consider the actual size of the beam. These solutions will be useful for effects in the center of the beam if the diffusion length is small compared to the beam radius, or if for times up to and including the melt-through time t_f the beam radius R is

$$R > 2\sqrt{\kappa t_f}.$$

In terms of the parameter τ_f this becomes, upon squaring both sides,

$$\tau_f < \frac{1}{4}\left(\frac{R}{\ell}\right)^2.$$

4. EFFECTS OF PULSED LASER RADIATION

4.1. Power Levels of Pulsed Lasers

Highly intense pulses of short duration can be produced in a variety of ways. Typically it is done by creating a large population inversion by the injection of electrical energy from the discharge of large, highly charged capacitors. In these systems all the energy is produced in a burst, the duration of which can be made quite short. We shall not discuss the various techniques by which these pulses are created, but in Table 4 we simply note some commonly obtained values [2].

Table 4

Laser Type	Pulse Length	Power	Energy Per Pulse
Ruby (normal mode)	0.1-1 ms	10-100 kW	1-50 J
Ruby (Q-switched)	10^{-8} s	1-10 GW	1-10 J
Ruby (mode-locked)	10^{-11} s	0.1-1 TW	0.1-1 J
CO_2 TEA	10×10^{-6} s	100 MW	100 J
CO_2 e-beam	2×10^{-5}	50 MW	1000 J
CO_2 shock tube gdl	3×10^{-4} s	0.3 MW	100 J

From the above table it is apparent that with beam areas of the order of 1 cm^2 extremely high power densities can be obtained, and, although the pulse lengths are short, the total energy in each pulse is considerable. The available power densities range as high as 10^{12} W/cm^2.

Practically speaking, one is usually interested only in power densities below the breakdown threshold of air because at higher power densities the energy never reaches the target. These breakdown levels are functions of wavelength, spot size, and pulse length, and depend as well on the contaminants in the air. Typical values are 10^9 W/cm^2 in "clean" air at STP for CO_2 laser pulses with duration of about 10^{-6} s and longer. At shorter pulse lengths the threshold is somewhat higher, becoming 10^{10} W/cm^2 at 10^{-8} s

and 10^{11} W/cm^2 at 10^{-10} s. In the infrared region, the breakdown threshold scales with the square of the frequency.

4.2. Material Vaporization Effects

We shall first discuss the effect of high-power-density laser pulses on materials from the point of view of target vaporization, and shall assume that the vaporizing surface is not shielded from the radiation by the vapor. In this case we can show that, in addition to thermal input to the target, there is a strong pressure built up on the target surface due to recoil from the blowoff of the vapor. The integral of this pressure over the time of the laser pulse imparts a net impulse to the target. There arises then the possibility of inducing stresses large enough to create gross mechanical changes, such as spall and deformation, by pulsed laser irradiation.

To calculate the pressure applied to a surface by a laser pulse, we start with a consideration of the vaporization process. We use a one-dimensional calculation because in most cases of interest the beam radius R is larger than the thermal diffusion length during the pulse time t_p, or

$$R \gg 2\sqrt{\kappa t_p} .$$

We shall avoid consideration of thin targets, so that ℓ is also large compared to the diffusion length. In this case we can calculate the time t_b required for the front surface to reach the vaporization temperature T_v from the semi-infinite slab result of Eq. (46), which is

$$T_v = \frac{2F_0}{K} \sqrt{\frac{\kappa t_b}{\pi}}$$

or

$$t_b = \frac{\pi K^2 T_v^2}{4 F_0^2 \kappa}$$

or, since

$$\kappa = \frac{K}{\rho C},$$

$$t_b = \frac{\pi}{4} \frac{K\rho C T_v^2}{F_0^2} . \tag{68}$$

In applying Eq. (46) in this way, we ignore the molten layer and assume that the values of K, ρ, and c appropriate to the solid can be used. This is not as gross an approximation as it may seem, because at these power densities the molten layer is very thin.

Once the material on the surface reaches the boiling point, the surface begins to erode at a rate U_s given by energy consideration, as we saw in section 3.

$$U_s = \frac{F_0}{\rho_s[C_{\text{solid}}T_m + L_m + C_{\text{liquid}}(T_v - T_m) + L_v]}$$

To simplify the calculation we take $C_{\text{liquid}} = C_{\text{solid}} = C$ and ignore L_m by comparison to L_v. Then

$$U_s = \frac{F_0}{\rho_s(L_v + CT_v)} . \tag{69}$$

Here we have used ρ_s for the density of the solid. So after the time t_b given by Eq. (68) the surface begins to evaporate, and it recedes at the rate U_s. By conservation of momentum it must be true that

$$\rho_v U_v = \rho_s U_s \tag{70}$$

where ρ_v and U_v designate the density and velocity, respectively, of the evaporation products. Thus we have

$$\rho_v U_v = \frac{F_0}{L_v + CT_v} \tag{71}$$

by combining Eqs. (69) and (70).

To see how the pressure exerted on the surface is related to density and velocity, note that the pressure on the surface is just the pressure of the evaporation products. To calculate this pressure, consider particles which move a distance Δz in time Δt under the pressure P and thereby acquire a velocity V. The pressure (force per unit area) must equal the rate of change of momentum (per unit area) so that

$$P = \frac{(\rho \Delta z) V}{\Delta t} .$$

That is, $\rho \Delta z$ is the mass per unit area which is brought to velocity V in time Δt by the force per unit area P. $V = \Delta z/\Delta t$, and so $P = \rho V^2$. Thus, in our specific case of density ρ_v and velocity U_v there is an associated pressure, given by

$$P = \rho_v U_v^2 . \tag{72}$$

We could compute the pressure from this expression if we knew ρ_v and U_v. However, we only know the product $\rho_v U_v$, from Eq. (71). We need another relationship, which we simply take from the ideal gas law,

$$P = \rho_v \frac{R}{A} T_v$$

where R is the gas constant and A the molecular weight. Denote R/A by $\mathcal{C}'$ and use Eq. (72), then

$$\rho_v U_v^2 = \rho_v \mathcal{C}' T_v$$

or

$$U_v = \sqrt{\mathcal{C}' T_v}.$$ (73)

Upon combining Eqs. (71) through (73), we get the desired relationship,

$$P = \frac{F_0 \sqrt{\mathcal{C}' T_v}}{L_v + C T_v}.$$

Since the specific heat of metal is typically $3R/A$ we can approximate $\mathcal{C}'$ by $(1/3) C$ to yield

$$P = \frac{1}{\sqrt{3}} \frac{F_0 \sqrt{C T_v}}{[L_v + C T_v]}.$$ (74)

Finally, we compute the specific impulse delivered during the pulse, which is the force per unit area multiplied by the time over which it acts, and we get

$$I_m = P(t_p - t_b)$$

or

$$I_m = \frac{1}{\sqrt{3}} \frac{F_0 \sqrt{C T_v}}{[L_v + C T_v]} \left(t_p - \frac{\pi}{4} \frac{K \rho C T_v^2}{F_0^2} \right).$$ (75a)

In terms of the energy in the pulse, $E_0 = F_0 t_p$, this can be written as

$$I_m = \frac{1}{\sqrt{3}} \frac{E_0 \sqrt{C T_v}}{[L_v + C T_v]} \left(1 - \frac{\pi}{4} \frac{K \rho C T_v^2}{E_0^2} t_p \right).$$ (75b)

A word about units is in order. It has become conventional to quote impulse in units of dyne-s, and specific impulse in dyne-s/cm^2. If we use J/cm^2 for energy density, J/g-°C for specific heat, and J/g for heat of vaporization, we have

$$[I_m] = \frac{\text{J/cm}^2}{\sqrt{\text{J/g}}}$$

$$= \text{cm}^{-2} \sqrt{\text{J-g}}$$

$$= \text{cm}^{-2} \sqrt{10^7 \text{ erg g}}$$

or

$$[I_m] = \sqrt{10^7} \text{ (dyne-s)/cm}^2.$$

This unit, dyne-s/cm^2, is called a tap. Thus, in taps,

$$I_m = 1.83 \times 10^3 E_0 \; \frac{\sqrt{CT_v}}{[L_v + CT_v]} \; \left(1 - \frac{\pi}{4} \frac{K\rho CT_v^2}{E_0^{\;2}} t_p\right). \tag{76}$$

Note that Eq. (76) predicts a threshold value of E_0 for impulse production at a given pulse length t_p. This is due to the criterion we introduced for vaporization; vaporization must commence before the end of the pulse or there will be no impulse. The threshold is given by

$$\frac{\pi}{4} \frac{K\rho CT_v^2}{E_0^{\;2}} t_p = 1$$

or

$$E_0)_{\text{th}} = \frac{\sqrt{\pi}}{2} T_v \sqrt{K\rho Ct_p}.$$

This vaporization model also predicts that, at very large E_0, the impulse per unit area is directly proportional to the energy density with a constant *coupling coefficient*, given by

$$\left(\frac{I_m}{E_0}\right)_{\text{max}} = 1.83 \times 10^3 \; \frac{\sqrt{CT_v}}{(L_v + CT_v)}.$$

This is the limit at which vaporization begins essentially instantaneously with respect to the pulse length and vapor products are produced for the entire pulse.

Some numerical values are illustrated below and in Fig. 35. E_0 is in J/cm^2 and t_p in μs, so that I_m is in taps:

For titanium

$$I_m = 8.04 E_0 \left[1 - 6.23 t_p/E_0^{\;2}\right].$$

For aluminum

$$I_m = 6.94 E_0 \left[1 - 33.9 t_p/E_0^{\;2}\right].$$

The above model illustrates the principles involved in generating impulse by laser vaporization. In fact, in predicting threshold values it gives results which are within a factor of two of experimental measurements. It has been refined [10] by a calculation which accounts for the fact that T_v is probably not a handbook value that comes from measurements at atmospheric pressure, but rather a different value appropriate to the dynamic and high-pressure situation created by the laser-induced vaporization. In this refinement, T_v is determined from the kinetic model of vaporization, which predicts that $U_s = c_a \exp\left[-L_v/(R'T_v)\right]$, where c_a is the speed of sound in the solid and R' the gas constant per gram. When this is done, the thresholds agree very well with theory. However, as E_0 (and hence F_0, since t_p is constant) is increased, experiments show that delivered impulse does not increase indefinitely but begins to fall off. This is due to the onset of absorption of laser energy by the vapor products and/or the heated air near the target. We turn now to a consideration of this problem.
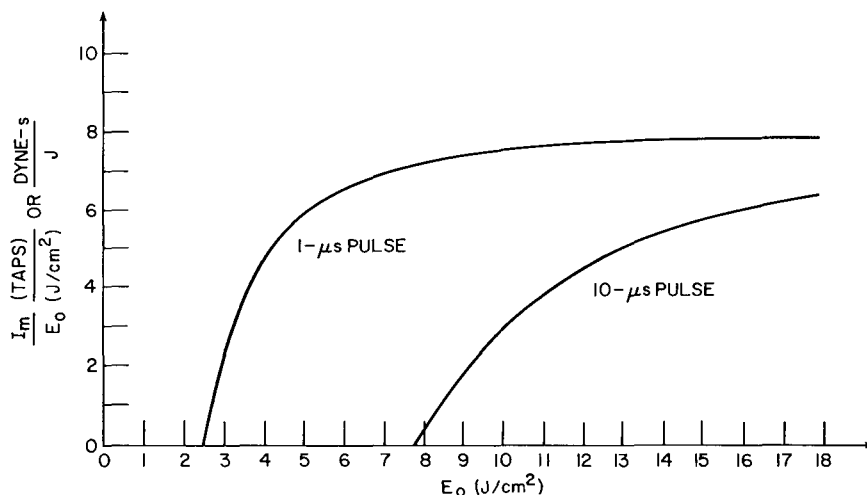
Fig. 35—Coupling coefficient vs energy density for titanium

4.3. Effects from Absorption of Radiation in the Plume

The plume of vaporized material blown off the target becomes, at some power density, hot enough that it or the air begins to absorb the laser radiation. The onset of this process is not thoroughly understood, and the ignition of these so-called absorption waves is the subject of a great deal of research. Proper treatment of the problem depends on, among other things, computing the onset of ionization and the rate of absorption of light by the electrons and also accounting for both cascade processes and relaxation processes in a full dynamic sense. We shall not treat this problem here. Rather we shall look at some crude models which show, in a semiquantitative way, various features of the absorption process.

First note that the decoupling of the absorption from the material surface due to shielding by the plume depends on the wavelength of the radiation. Recall from Eqs. (34) that at the plasma frequency the reflectivity of a "free-electron" metal drops sharply from a value near unity to essentially zero. If we assume that the coupling to the plume is due to the light interacting with electrons, Eq. (34a) is valid. Using the mass of the free electron gives

$$\nu_p = 8.97 \times 10^3 N^{1/2} \tag{77}$$

for the plasma frequency in hertz, when N is in electrons per cubic centimeter. This can be rewritten in terms of the corresponding wavelength λ_p to yield

$$N = (1.12 \times 10^{13}) / \lambda_p^2 \tag{78}$$

where λ_p is in centimeters. At a given wavelength the plume is transparent until the electron density reaches the value given by Eq. (78), where there will be a transition to a condition in which the plume absorbs and reflects the radiation and thereby shields the material. For 10.6-μm (CO_2) radiation, shielding begins at 10^{19} electrons per cm^3, for

58

1.06 μm (Nd) at 10^{21} electrons per cm^3, and for 0.6943 μm (ruby) at 2.3×10^{21} electrons per cm^3.

When the electron density reaches a high enough value, the beam decouples from the surface and presumably the pressure due to material blowoff will drop. To get some idea of the order of magnitude of the energy density for a given pulse length where this process begins, let us simply assume that cutoff begins when the front surface reaches the temperature at which the material is fully ionized. This should predict an upper limit, for full ionization is obviously not required. For example, solids have $N \approx 10^{23}$ cm^{-3}, whereas we only require, at 10.6 μm, $N > 10^{19}$ cm^{-3}. For simplicity assume that melting and vaporization processes can be ignored, and again use for the front surface temperature rise the simple expression

$$T = \frac{2F_0}{K} \sqrt{\frac{\kappa t}{\pi}}.$$

A typical ionization temperature for a metal would be about 75,000°C. Using simply the values of K and κ for the solid, we get for titanium,

$$F_0 \sqrt{t} \approx 5.7 \times 10^4 \text{ W s}^{1/2}/\text{cm}^2 .$$

Using $E_0 = F_0 t$, this can be rewritten as

$$E_0 \approx 57 \sqrt{t_{\mu s}} \tag{79}$$

where $t_{\mu s}$ is understood to be time in microseconds.

Figure 36 shows some data taken by Dr. Rudder of the Air Force Weapons Laboratory, at two pulse lengths, 1.2 and 11 μs, with 1.06-μm radiation and titanium targets [11]. The lines marked "Anisimov predictions" are calculated from the vaporization model of the previous section with the refined method for determining T_v. (This was first done in the Soviet Union by Anisimov [19].) The experimental data agree very well at values of E near threshold. Note that Eq. (79) for estimating the onset of shielding is roughly consistent with these data, although the experimental onset of shielding is, as one might expect, fairly gradual. The line on the graph marked LSD Predictions refers to a theoretical estimate based on the idea that the laser light, when it couples into the blowoff, can create an explosionlike shock wave in the air which travels up the beam, absorbing the radiation energy in the process. This laser-supported-detonation, or LSD, wave is one form of laser-supported-absorption wave. We will discuss these waves next.

Once the coupling of the radiation with the ejected vapor (and perhaps the air) reaches a sufficient level, the absorption region begins to behave in a fashion characterized by hydrodynamic dissipation of the energy coupled into it. For now, let us ignore the ignition problem. The absorption region typically propagates up the laser beam in a way that is determined by the medium in which it propagates (usually air) and also by the balance between the power being fed in by the laser and the relaxation processes which dissipate the power. Three types of laser-supported-absorption waves are usually identified. Typical power levels at which they appear and their typical velocities of propagation are indicated below for 10.6-μm radiation and targets in air at standard temperature and pressure [12].
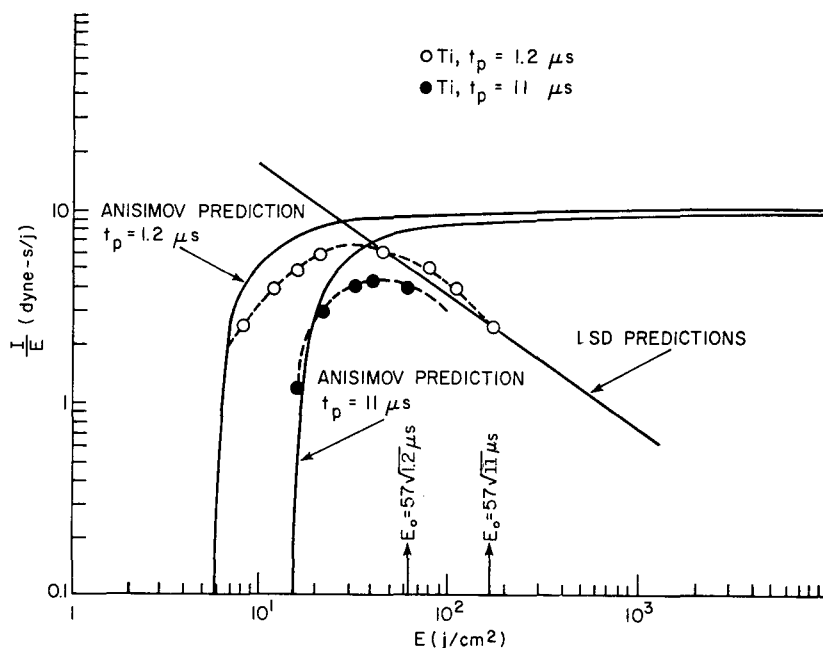
Fig. 36—Specific impulse delivered to solid targets by 1.06-μm laser radiation (Ref. 11)

Type of Wave	Power Level of Laser Flux (W/cm^2)	Velocity of Propagation (cm/s)
Laser-supported-detonation wave (LSDW)	10^7	10^5
Laser-supported-combustion wave (LSCW)	10^4	10^3
Plasmatron	10^4	0

The LSD wave propagates as a shock wave, i.e., at supersonic velocity, whereas the LSC wave moves more slowly and relaxes by thermal conduction. The plasmatron is at rest, with the energy input being balanced by reradiation and convective losses into the atmosphere. Although we discuss these effects here in the section on pulsed lasers, they are just as valid for continuous radiation. Since pulsed lasers are the most convenient devices for reaching these power levels, especially for LSD waves, absorption waves are usually considered under pulsed effects.

Hydrodynamic theory can be applied to model these waves. The problem was first solved in the Soviet Union by Raizer [13]. Detonation waves can be discussed most readily because the hydrodynamic equations reduce to fairly simple expressions, so we shall consider them in some detail. A few remarks about combustion waves will come later.

60

We can derive conditions for the steady-state behavior of a detonation wave by considering conservation of mass, momentum, and energy at the detonation front. For this purpose we do not concern ourselves with how the process starts but presume that a detonation wave has been formed and is propagating at some steady rate as sketched in Fig. 37. The absorption region is propagating to the right at a steady velocity u. We assume that it is very thin and can be treated as a detonation front. Thus u is the detonation velocity. The temperature and density, etc., of the air go through very rapid changes in the very short distance ℓ. Note that this wave propagates, in this treatment, in air, and thus our results will be independent of target material.
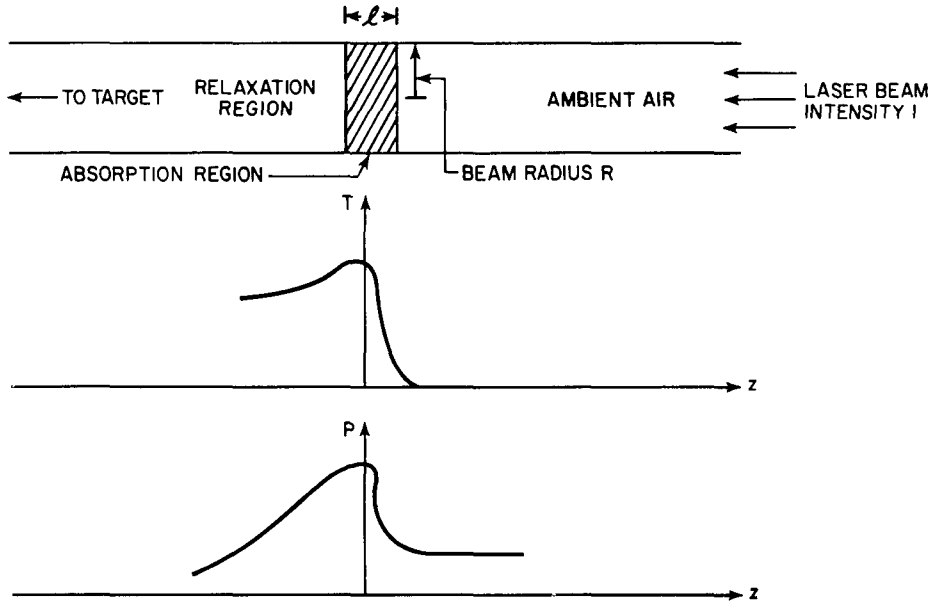

Fig. 37—Temperature and density profiles typical of a
laser-supported-detonation wave (Ref. 12)

In this discussion "behind the front" refers to the high-temperature-and-pressure region immediately to the left of the absorption region in Fig. 37. "Ahead of the front" is to the right in the sketch and refers to ambient air conditions. Note we have given the beam a finite radius R and thus will have to consider lateral expansion. First let us do the one-dimensional problem and assume that the detonation front propagates simply as a plane wave.

Behind the front let ρ, P, and e be the density, pressure, and internal energy *per unit mass*, respectively, and let ρ_0, P_0, and e_0 be the same variables ahead of the front. Define the velocities with respect to a coordinate system moving with the front at the detonation rate u. Then the ambient gas moves into the front with the speed u, and we define v as the speed with which the high-pressure gases leave the front. We can now write down the conservation equations for mass, momentum, and energy across the detonation front. These equations are based on *flow*, that is, they are in the terms of "per unit area, per unit time." The equation for mass is

Mass

$$\rho_0 u = \rho v. \tag{80}$$

The conservation-of-momentum condition results from equating the impulse to the change in momentum. Now impulse is force multiplied by time, but in the "per unit area, per unit time" sense this becomes simply pressure. Since mass, in this flow concept, is ρv, momentum is $(\rho v)v$. Hence we have

$$P - P_0 = -[(\rho v)v - (\rho_0 u)u] \,,$$

and, if we ignore P_0, which is much smaller than P, we have for momentum

Momentum

$$P + \rho v^2 = \rho_0 u^2 \,. \tag{81}$$

The conservation-of-energy condition follows from similar considerations. The difference in energy flow on each side of the front must be balanced by the work done on the gas $(P_0 u - Pv)$ and the energy absorbed from the laser beam, which, using our earlier notation, is F. $F = \mathcal{C}I$, where $\mathcal{C}$ is the absorptance of the gas in the absorption region.

Thus we have

$$\rho v \left(e + \frac{1}{2} v^2\right) - \rho_0 u \left(e_0 + \frac{1}{2} u^2\right) = P_0 u - Pv + F \,.$$

If we use $P_0 \approx 0$ and $e_0 \approx 0$ and substitute from Eq. (80), we get for energy

$$e + \frac{1}{2} v^2 - \frac{1}{2} u^2 = -\frac{P}{\rho} + \frac{F}{\rho_0 u}$$

or

Energy

$$e + \frac{P}{\rho} + \frac{1}{2} v^2 = \frac{1}{2} u^2 + \frac{F}{\rho_0 u} \,. \tag{82}$$

Our goal is to use these conservation laws to predict the pressure P behind the front and ultimately the pressure transmitted to the target. For now assume that F is known, and, of course, the ambient air density ρ_0 is known. Thus we have three equations and five unknowns, P, ρ, v, e, and u. To proceed we need to invoke some equation of state for the gases, and we shall simply assume that the ideal gas law holds. Thus we have

$$P = \rho R'T \tag{83}$$

where R' is the gas constant per unit mass, or $R' = R/A$, where A is the molecular weight. (Since the wave is presumed to be in air in this treatment, A would be the average molecular weight of air. Taking A for air to be 29.4 g/mol gives $R' = 2.84 \times 10^6$ erg/(g-°C) and is consistent with the ideal gas law and with $\rho_0 = 1.29 \times 10^{-3}$ g/cm^3 for air at 0°C and 1 atmosphere = 10^6 dyne/cm^2.) Now Eq. (83) essentially introduces another unknown, the temperature T, so we need to add the expression for the energy of an ideal gas, which is

$$e = \frac{R'T}{\gamma - 1} = \frac{P}{(\gamma - 1)\rho} \tag{84}$$

where γ is the ratio of the specific heats, $\gamma = C_p/C_v$. For our purposes it is sufficient to take $\gamma = 1.4$.

Now we have four equations (Eqs. (80)-(82), (84)) in five unknowns (P, ρ, v, e, and u). To get the final condition we use the criterion for detonation, which is that the velocity of the high-pressure gases behind the front, relative to the front, is equal to or greater than the local speed of sound. Intuitively this seems reasonable, for propagation of shock waves is, by definition, in excess of the speed of sound. The criterion can be properly derived from a consideration of the thermodynamics of the situation, but we shall not do so here [14]. Since we shall be interested in the minimum value of I (or F) required to sustain a detonation wave, we take v equal to the speed of sound. For an ideal gas the sound speed is $(\gamma P/\rho)^{1/2}$, so we have our last condition,

$$v^2 = \frac{\gamma P}{\rho}. \tag{85}$$

Before discussing the algebra, let us collect the equations—

$$\rho_0 u = \rho v \tag{80}$$

$$P + \rho v^2 = \rho_0 u^2 \tag{81}$$

$$e + \frac{P}{\rho} + \frac{1}{2} v^2 = \frac{1}{2} u^2 + \frac{F}{\rho_0 u} \tag{82}$$

$$e = \frac{P}{(\gamma - 1)\rho} \tag{84}$$

$$v^2 = \frac{\gamma P}{\rho}. \tag{85}$$

Combine Eqs. (80) and (81) to yield expressions for u^2 and v^2:

$$u^2 = \frac{P\rho}{\rho_0(\rho - \rho_0)} \tag{86}$$

$$v^2 = \frac{P\rho_0}{\rho(\rho - \rho_0)}. \tag{87}$$

Now use Eqs. (85) and (87) to eliminate v^2 and ρ so that we can get

$$\frac{\rho}{\rho_0} = \frac{1 + \gamma}{\gamma} \tag{88}$$

which is one of the equations we need, namely ρ in terms of the known quantities ρ_0 and γ. Now we can use Eq. (81) to get P in terms of u by eliminating v^2 with Eq. (85) to get

$$P = \frac{\rho_0 u^2}{1 + \gamma}. \tag{89}$$

We need one more relation to complete the solution, namely u in terms of F. This will, by Eq. (89), give us P in terms of F. To get this we use Eq. (82) and replace e via Eq. (84) and v^2 via Eq. (85). Thus Eq. (82) becomes

$$\frac{P}{(\gamma - 1)\rho} + \frac{P}{\rho} + \frac{1}{2} \frac{\gamma P}{\rho} = \frac{1}{2} u^2 + \frac{F}{\rho_0 u}.$$

If we use Eq. (89) to eliminate P, we get

$$\frac{u^2}{1 + \gamma} \left[\frac{1}{(\gamma - 1)} \frac{\rho_0}{\rho} + \frac{\rho_0}{\rho} + \frac{1}{2} \gamma \frac{\rho_0}{\rho} \right] = \frac{1}{2} u^2 + \frac{F}{\rho_0 u}$$

or

$$\left(\frac{\rho_0}{\rho} \right) \left(\frac{u^2}{1 + \gamma} \right) \left[\frac{\frac{1}{2} \gamma (1 + \gamma)}{\gamma - 1} \right] = \frac{1}{2} u^2 + \frac{F}{\rho_0 u}$$

or

$$\frac{1}{2} \frac{\rho_0}{\rho} u^2 \left(\frac{\gamma}{\gamma - 1} \right) = \frac{1}{2} u^2 + \frac{F}{\rho_0 u}.$$

If we use Eq. (88) for ρ_0/ρ, we get

$$\frac{1}{2} u^2 \frac{\gamma^2}{(\gamma^2 - 1)} = \frac{1}{2} u^2 + \frac{F}{\rho_0 u}.$$

Finally we arrive at

$$u^3 \left(\frac{1}{\gamma^2 - 1} \right) = \frac{2F}{\rho_0}$$

or

$$u = \left(\frac{2(\gamma^2 - 1)F}{\rho_0} \right)^{1/3}. \tag{90}$$

The equations which represent the solution for the detonation wave, then, are

$$\frac{\rho}{\rho_0} = \frac{1 + \gamma}{\gamma} \tag{88}$$

$$P = \frac{\rho_0 u^2}{1 + \gamma} \tag{89}$$

$$u = \left[\frac{2(\gamma^2 - 1)F}{\rho_0}\right]^{1/3} . \tag{90}$$

These three equations, together with the ideal gas law, represent the formal solution to the propagation of the laser-supported-detonation wave. Given the temperature behind the front, and since Eq. (88) defines ρ, we could calculate P and hence u and finally the F required to support it. However, this does not really solve the problem. What we wish to discover is: given the laser intensity I, will an LSD wave be supported? To answer this question, we need to consider the distance it takes for the laser radiation to be absorbed. We also need a more realistic situation then the simple plane wave.

First we note that the beam has a finite radius R and that lateral expansion can take place. The order of magnitude of the radial expansion velocity will be the speed of sound c_a. To maintain the detonation, we must replace the energy lost to expansion by energy put into the absorption region. To simplify, let us assume all of the laser beam energy is absorbed in the distance ℓ. (Actually the beam intensity only falls by $1/e$ in the distance ℓ.) We define Δt as the time for the shock front to move a distance ℓ, or $\Delta t = \ell/u$. In this time the radial expansion is the amount $c_a \Delta t$. Now $\pi R^2 I \Delta t$ is the energy deposited by the beam in the cylindrical volume shown in Fig. 38 ($c_a \Delta t \ll R$). But the energy in this volume after expansion is approximately equal to its volume multiplied by its internal energy per unit volume. Thus

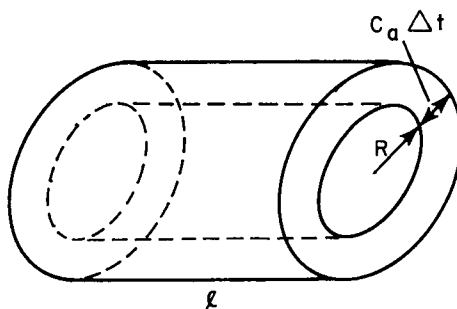$$\pi R^2 I \Delta t \approx \rho_0 e [\pi R^2 \ell + 2\pi R c_a \Delta t \ell] .$$

Fig. 38—Cylindrical volume which absorbs
beam energy via expansion

Since $\Delta t = \ell/u$,

$$I\pi R^2 \approx \rho_0 e u \left[\pi R^2 + 2\pi R c_a \frac{\ell}{u}\right] .$$

Note that for $\gamma \approx 1.4$, Eq. (88) predicts that $\rho. \approx 2\rho_0$ and hence, using $\rho v = \rho c_a \equiv \rho_0 u$, $u \approx 2c_a$. So we have, after some algebra,

$$\rho_0 e u \approx \frac{I}{1 + \dfrac{\ell}{R}} . \tag{91}$$

65

But this equation simply represents the rate at which we must put energy into the absorption volume in order to maintain the conditions we assume to carry out our detonation wave calculation, namely a plane wave propagating by absorption of laser energy in a distance ℓ. Thus the energy flow per unit area from the laser beam is

$$F = \frac{I}{1 + (\ell/R)} .$$ (92)

Finally, we can complete the problem if we know the absorption length ℓ. To compute ℓ we need to invoke some model of the ionized air. For this purpose it is sufficient to assume that free electrons absorb the light and that the electrons come from singly ionized atoms. We shall not derive the expressions which we need but simply quote them. There are two relationships. The first of these is the Saha equation [14a], which relates the fraction of atoms ionized α to the absolute temperature T and the ionization potential $\mathcal{I}$ of a single atom:

$$\frac{\alpha^2}{1 - \alpha} = 2 \frac{g_1}{g_0} \frac{m}{\rho} \left(\frac{2\pi m_0 kT}{h^2}\right)^{3/2} e^{-\mathcal{I}/kT} .$$ (93)

In this equation m is the mass of the atom, m_0 is that of the electron, k is Boltzmann's constant, and h is Planck's constant. The statistical weights of the ground state of the atom and its first ionized state are g_0 and g_1, respectively. Typically $g_1 = g_0 = 1$. In terms of known constants, then, the Saha equation gives us the degree of ionization as a function of temperature.

Knowing the degree of ionization, we can get the absorption length. Again we simply quote the relationship [12], which assumes that the light is absorbed by inverse bremsstrahlung. The expression is

$$\frac{1}{\ell} = \frac{4}{3} \left(\frac{2\pi}{3m_0 kT}\right)^{1/2} \frac{e^6 h^2}{m_0 c (h\nu)^3} \left(\frac{\rho^2 \alpha^2}{m^2}\right) (1 - e^{-h\nu/kT})$$

which, at the temperatures of interest and for 10.6-μm radiation, becomes (for $h\nu/kT \ll 1$)

$$\frac{1}{\ell} = \frac{4}{3} \left(\frac{2\pi}{3m_0}\right)^{1/2} \frac{e^6 h^2}{m^2 m_0 c (h\nu)^2} \cdot \frac{\rho^2 \alpha^2}{(kT)^{3/2}} .$$ (94)

In Eq. (94) ν is, of course, the frequency of the laser radiation, c is the speed of light, and e is the electronic charge. By combining Eqs. (93) and (94) we can calculate ℓ in terms of temperature T, density ρ, and known parameters. A typical value of $\mathcal{I}$ for air is of the order of 13 eV. (For O_2 $\mathcal{I}$ is 12.1 eV, for N_2 it is 15.6 eV.) Thus we have

$$\ell = f(\rho, T)$$

or, since $\rho = \rho_0(1 + \gamma)/\gamma \approx 2\rho_0$, we can get a relationship between ℓ and T and hence between I and T, via Eqs. (90) and (92). Typical results are shown in Fig. 39.
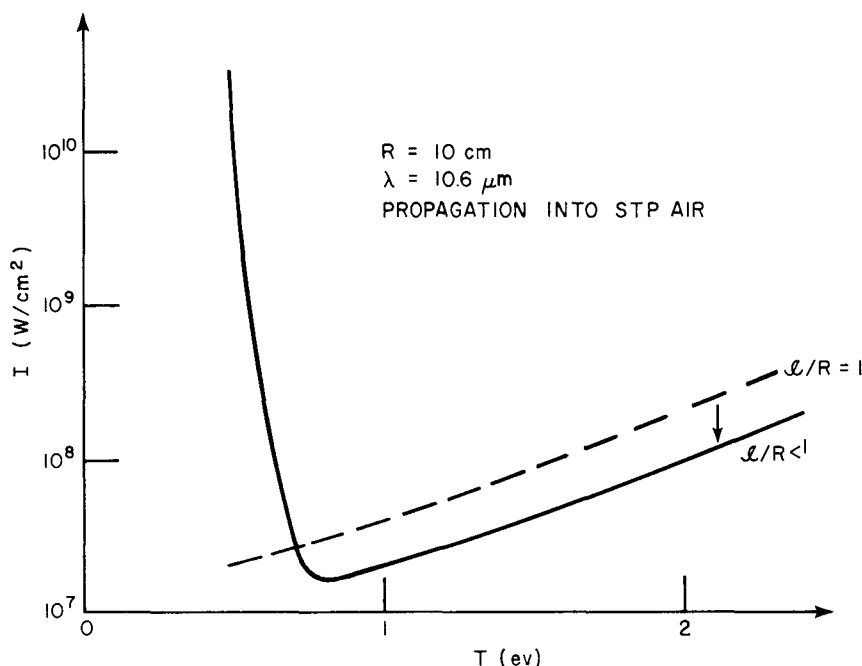
Fig. 39—Relationship between I and T for a laser-supported-detonation wave (Ref. 12). This plot is based on a more realistic expression for the equation of state of the gases than the ideal gas law, but the ideal gas law gives a similar result.

Here we have assumed a beam radius of 10 cm. The important point is that there is a *minimum* in the I-vs-T relation. We identify this as the minimum flux I_m required to maintain an LSD wave. Associated with it is the temperature T_m of the high-pressure region at the detonation front. We can then use our detonation-wave relationships, Eqs. (88) through (90), to get the pressure behind the front, or equivalently, get pressure from T_m via $\rho \approx 2\rho_0$ and the ideal gas law.

We shall turn to a calculation of the pressure on the target in a moment. First note that the radial expansion concept imposes a natural criterion for the difference between a combustion wave and a detonation wave. The time for radial expansion is R/c_a whereas the time for passage of the absorption region is ℓ/u. If the detonation condition is to be maintained, radial expansion times must be larger than propagation times in order for the high-pressure region to move as a shock front and not dissipate itself radially. Hence $R/c_a > \ell/u$. We have already noted that $u \approx 2c_a$ or, crudely, $u \approx c_a$, so that $R > \ell$, or $\ell/R < 1$, is the condition for detonation waves. If ℓ becomes larger than R the absorption region is large, the relaxation in the radial direction is important, and the process called a combustion wave takes place. This can be treated in a similar fashion to the detonation wave, but the hydrodynamic equations do not take the simple form of Eqs. (80)-(82). We shall not treat combustion waves in this report. The solution in Fig. 39 is for a detonation wave and hence is valid for $\ell/R < 1$. The limit $\ell/R = 1$ is shown in the figure by a dashed line.

Finally, compute the impulse delivered to a target by a laser beam of intensity I just sufficient to maintain a detonation wave [11]. The beam has a pulse duration t_p. We wish to calculate the effect on the target due to the "explosion products" behind the

absorption region. These, of course, expand in all directions and create a pressure on the target. To demonstrate the effect we shall use a very simple model, namely a model of cylindrical expansion. We consider that the absorption region has propagated a distance Z by the end of the laser pulse, and at that time we have created a cylinder of high-pressure gas which has a radius equal to the beam radius R, a length Z, and a pressure P_d given by Eqs. (89) and (90) above, with $P = P_d$. This cylinder is then allowed to expand radially at a speed estimated to be the speed of sound c_a. Then we get the impulse delivered to the target by integrating the force on the target due to the pressure in the expanding cylinder during the time the cylinder expands from R to the target radius R_T. For R_T very large, the integration is stopped when the cylinder pressure drops to atmospheric pressure. The model is sketched in Fig. 40 at the time $t = t_p$.
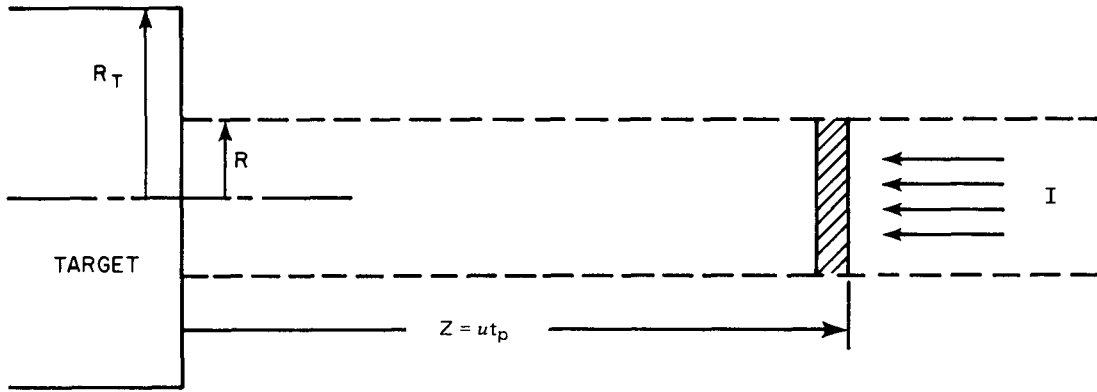

Fig. 40—Radial expansion model for impulse delivered to a target from a laser-supported-detonation wave

The model might be expected to be valid if $Z >> R$ and if $t_p <<$ the time required for radial expansion, either to R_T or to atmospheric pressure, to take place. We also are assuming that impulse due to target vaporization is negligible, i.e., that the detonation wave is formed very early in the laser pulse.

We take the radial expansion to be at constant temperature. Then P times the volume $\mho$ of the cylinder is a constant. Since our model presumes only cylindrical expansion, we have the condition that

$$Pr^2 = \text{constant} \tag{95}$$

where r is the radius of the cylinder and $R \leqslant r \leqslant R_T$. We shall need this relationship in the derivation of the impulse. Let the impulse be I'_m, and let F be the force on the target due to the pressure. This gives

$$I'_m = \int_{t(r=R)}^{t(r=R_T)} F \, dt$$

where the upper limit is understood to be valid only where P is greater than atmospheric pressure at $r = R_T$. Since the radial expansion rate is c_a

$$dr = c_a \, dt.$$

From ideal gas relation for the speed of sound,

$$c_a = \sqrt{\frac{\gamma P}{\rho}},$$

we have

$$dt = \sqrt{\frac{\rho}{\gamma P}} \, dr.$$

Thus

$$I'_m = \int_R^{R_T} F \sqrt{\frac{\rho}{\gamma P}} \, dr.$$

Now at any time

$$F = (\pi r^2) P,$$

but, since $r^2 P$ is constant, we can evaluate F from the initial pressure P_d at $r = R$, or

$$F = \pi R^2 P_d.$$

Now the impulse becomes

$$I'_m = \pi R^2 P_d \int_R^{R_T} \sqrt{\frac{\rho}{\gamma P}} \, dr.$$

Again invoking $r^2 P = $ constant gives

$$r^2 P = P_d R^2$$

or

$$P = P_d \frac{R^2}{r^2}.$$

So the impulse is

$$I'_m = \pi R \sqrt{P_d} \int_R^{R_T} \sqrt{\frac{\rho}{\gamma}} \, r dr. \tag{96}$$

Recall from Eq. (88) that $\rho = \rho_0 (1 + \gamma)/\gamma$. This gives

$$I'_m = \pi R \sqrt{\frac{P_d \rho_0 (1 + \gamma)}{\gamma^2}} \left(\frac{R_T^2}{2} - \frac{R^2}{2} \right).$$

Since $R < R_T$, we shall ignore the $R^2/2$ term. The specific impulse I_m, which is I'_m divided by the area of the laser beam πR^2 is then

$$I_m = \frac{R_T^2}{2R} \sqrt{P_d \rho_0} \frac{\sqrt{1+\gamma}}{\gamma}.$$

Recalling the expression in Eqs. (89) and (90) for P_d, and ignoring ℓ/R with respect to unity, we can write

$$I_m = \frac{R_T^2}{2R} \sqrt{\left(\frac{1+\gamma}{\gamma^2}\right) \rho_0 \left(\frac{\rho_0}{1+\gamma}\right) \left[\frac{2(\gamma^2-1)}{\rho_0} I\right]^{2/3}}.$$

This simplifies to

$$I_m = \frac{R_T^2}{2R} \left\{\frac{1}{\gamma} [2(\gamma^2-1)]^{1/3}\right\} \rho_0^{2/3} I^{1/3}.$$

The expression in braces is nearly equal to unity for typical value of γ (say, $\gamma = 1.4$), so

$$I_m = \frac{R_T^2}{2R} \rho_0^{2/3} I^{1/3}.$$

Now the energy per unit area in the beam is $E_0 = I t_p$, and we can write the coupling coefficient I_m/E_0 as

$$\frac{I_m}{E_0} = \frac{R_T^2}{2R} \rho_0^{2/3} \bigg/ \left(t_p^{1/3} E_0^{2/3}\right). \tag{97}$$

This is the equation of the straight line marked LSD Predictions shown in Fig. 36, where the calculations were done for the parameters appropriate to the 1.2-μs pulse length.

Several important consequences of the LSD wave are seen in Eq. (97). One is that the coupling coefficient is reduced as E_0 becomes larger, which tells us that we cannot create an arbitrarily large impulse at a target by simply increasing the energy in the laser beam. In fact, when Eq. (97) is considered to be correct at high E_0 and the results of the vaporization model (see Eq. (76) and Fig. 36) are used at lower values of E_0, there is, for a given pulse length, an optimum value of E_0 for transferring the largest amount of impulse to a target. For the 1.2-μs pulse illustrated in Fig. 36 the optimum value of E_0 is about 22 J/cm^2, and this is in reasonable accord with the data. Of course the specific impulse I_m per se goes as $E_0^{1/3}$, so larger E_0 will create larger I_m. However, this slow increase of I_m with E_0 is a very inefficient way to impart stress to a material. A better scheme, perhaps, would be to use multiple pulses at the optimum E_0 value.

Another consequence of the LSD wave is a lack of dependence of impulse on the parameters of the target material. The same impulse is produced independently of the

target. This is in accord with experiment. When I is well into the range where LSD's are formed, the measured impulse is the same for all target materials. Some data taken by NRL [15] are shown in Fig. 41. In this graph we see, in accord with the vaporization model, a strong dependence of I_m/E_0 on material type at lower power densities, whereas at the high power densities typical of LSD formation the values of I_m/E_0 are the same for all materials. In this range, however, a target area dependence appears. The target area dependence shown is for aluminum. Here again the general behavior predicted by Eq. (97) can be seen.
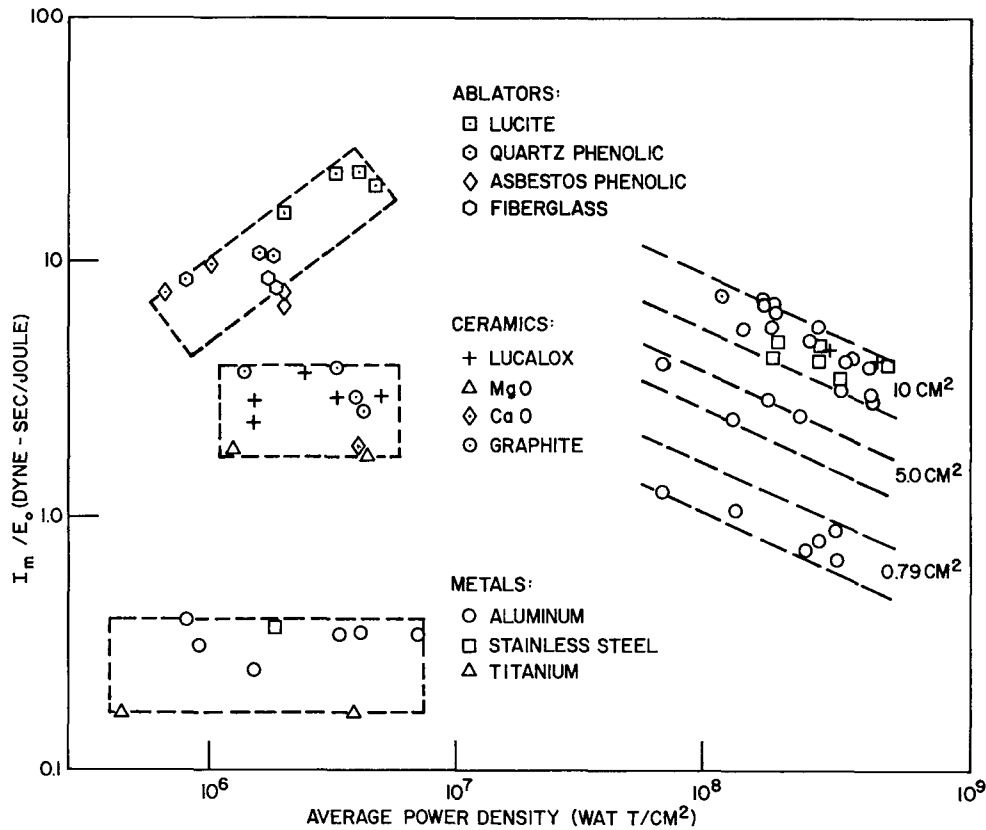

Fig. 41—Coupling coefficient as a function of power density (Ref. 15)

We have not yet considered the radius at which the expanding cylinder reaches atmospheric pressure. Call this radius R_0. As explained above Pr^2 is constant, so

$$P_0 R_0^2 = P_d R^2$$

where P_0 is atmospheric pressure, 10^6 dyne/cm^2. Thus,

$$R_0 = R P_0^{-1/2} P_d^{1/2} .$$

From Eqs. (89) and (90), for P_d this becomes

$$R_0 = RP_0^{-1/2} \sqrt{\frac{\rho_0}{1 + \gamma} \left[\frac{2(\gamma^2 - 1)I}{\rho_0} \right]^{2/3}} .$$

Again the factors involving γ are nearly unity, so

$$R_0 = RP_0^{-1/2} \rho_0^{1/6} I^{1/3} .$$

Upon substituting $I = E_0/t_p$, we get

$$R_0 = RP_0^{-1/2} \rho_0^{1/6} E_0^{1/3} t_p^{-1/3} . \tag{98}$$

So if R_0 is less than R_T, one replaces R_T by R_0 in Eq. (97). Target sizes larger than R_0 will all receive the same impulse.

A numerical illustration is useful. Let $E_0 = 1000$ J/cm^2 and $t_p = 100$ μs. Suppose the beam radius is 1 cm. The power density I is about 10^7 W/cm^2, so we expect a LSD wave. If we take $R_T = 5$ cm for the target radius, Eq. (97) yields (with $\rho_0 = 1.29 \times 10^{-3}$ g/cm^3)

$$\frac{I_m}{E_0} = \frac{5^2}{2} (1.29 \times 10^{-3})^{2/3} \Big/ \left[(10^{-4})^{1/3} (10^{10})^{2/3} \right] \frac{\text{dyne-s}}{\text{erg}}$$

$$\frac{I_m}{E_0} \approx 7 \times 10^{-7} \text{ dyne-s/erg}$$

or

$$\frac{I_m}{E_0} \approx 7 \text{ dyne-s/J} .$$

In this example expansion to atmospheric pressure would take place at a radius given by Eq. (98):

$$R_0 = (10^6)^{-1/2} (1.29 \times 10^{-3})^{1/6} (10^{10})^{1/3} (10^{-4})^{-1/3}$$

where we have used erg/cm^2 for E_0. Then

$$R_0 \approx 15 \text{ cm} .$$

Thus targets with radii of 15 cm and larger would exhibit a maximum coupling coefficient of $(15/5)^2$ times 7, or about 63 dyne-s/J. If we compute I_m, we have 63,000 dyne-s/cm^2, that is, 63,000 taps, as the maximum specific impulse from this laser pulse. Since this impulse is delivered in times of the order of magnitude of the laser pulse time, this corresponds to a pressure of roughly $(6.3 \times 10^4)/10^{-4} \approx 6 \times 10^8$ dyne/cm^2, or about 600 atmospheres.

REFERENCES

1. D. Röss, *Lasers: Light Amplifiers and Oscillators*, Academic Press, New York, 1969, p. 72.

2. John F. Ready, *Effects of High-power Laser Radiation*, Academic Press, New York, 1971.

3. T.J. Wieting and J.T. Schriempf, "Report of NRL Progress," June, 1972, pp. 1-13.

4. A.M. Bonch-Bruevich and Ya. A. Imas, *Zh. Tekh. Fiz.* 37, 1917 (1967); English transl.: *Sov. Phys.-Tech. Phys.* 12, 1407 (1968).

5. H.S. Carslaw and J.C. Jaeger, *Conduction of Heat in Solids*, 2nd ed., Clarendon Press, Oxford, 1959.

6. W.J. Parker, R.J. Jenkins, C.P. Butler, and G.L. Abbott, *J. Appl. Phys.* 32, 1679 (1961).

7. R.C. Heckman, "Thermal Diffusivity Finite Pulse Time Corrections," Sandia Laboratories Research Report SC-RR-710280, May 1971.

8. J.T. Schriempf, *Rev. Sci. Instr.* 43, 781 (1972).

9. G.E. Nash, "Thermal Response Calculations," Naval Research Laboratory, Washington, D.C., unpublished data.

10. S.I. Anisimov, *High Temperature* 6, 110 (1968). Translated from *Teplofizika Vysokikh Temperatur* 6, 116 (1968). Original article submitted December 6, 1966.

11. G.H. Canavan, P.E. Nielsen, and R.D. Harris, "Reduction of Momentum Transfer to Solid Targets by Plasma Ignition," Air Force Weapons Laboratory Laser Division Digest LRD-72-1, p. 125, June 1972.

12. P.E. Nielsen and G.H. Canavan, "Laser Absorption Waves," Air Force Weapons Laboratory Laser Division Digest LRD-71-2, p. 110, December 1971.

13. Yu. P. Raizer, *Soviet Physics JETP* 21, 1009 (1965).

14. Ya. B. Zel'dovich and Yu P. Raizer, *Physics of Shock Waves and High-Temperature Hydrodynamic Phenomena*, Academic Press, New York, 1966, p. 346.

    a. p. 195.

15. S.A. Metz, L.R. Hettche, and R.L. Stegman, "Intensity Dependence of Target Response to High-Intensity Pulsed 10.6-μ Laser Radiation," DOD Laser Effects/Hardening Conference, Monterey, Calif., 23-26 October 1973.